



Commission of the European Communities

COST

physical sciences

**Stress corrosion cracking
and corrosion fatigue of steam-turbine
rotor and blade materials**

Report

EUR 13186 EN



Commission of the European Communities

COST

**Stress corrosion cracking
and corrosion fatigue of steam-turbine
rotor and blade materials**

M. O. Speidel,¹ J. Denk,² B. Scarlin²

¹Institute of Metallurgy
CH-Eth, Zürich

²Asea Brown Boveri
CH-Baden

Edited by

J. B. Marriott

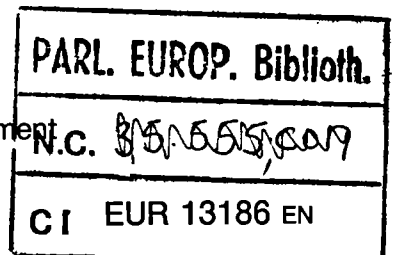
Commission of the European Communities

Contract No: ECI COST-0010-CH (CH)

Directorate-General
Science, Research and Development

1991

ms 76949



Published by the
COMMISSION OF THE EUROPEAN COMMUNITIES

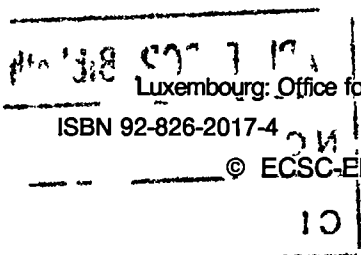
**Directorate-General
Telecommunications, Information Industries and Innovation**

L-2920 Luxembourg

LEGAL NOTICE

Neither the Commission of the European Communities nor any person acting on behalf of the Commission is responsible for the use which might be made of the following information

Cataloguing data can be found at the end of this publication



Luxembourg: Office for Official Publications of the European Communities, 1991

ISBN 92-826-2017-4

Catalogue number: CD-NA-13186-EN-C

© ECSC-EEC-EAEC, Brussels · Luxembourg, 1991

Printed in Germany

PREFACE

Stress Corrosion Cracking and Corrosion Fatigue of Steam Turbine Rotor and Blade Materials

Research on high temperature materials which are critical for the safe and efficient operation of power engineering equipment has been an important feature of COST concerted action programmes for the last eighteen years; starting with COST 50; "Materials for Gas Turbines".

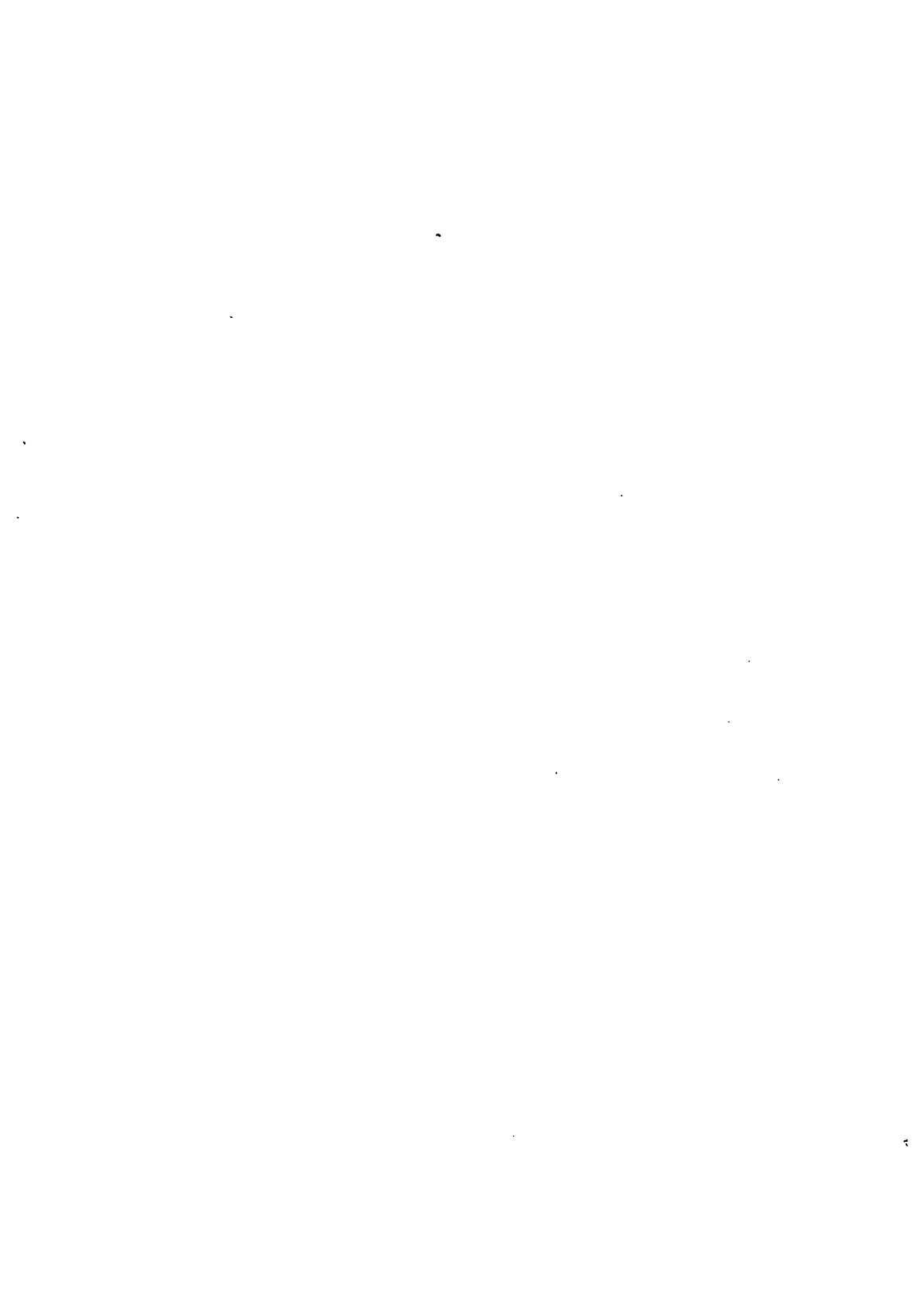
In recent years specific attention, has been devoted to "Materials for Steam Turbines" - COST 505. The countries represented in this work have been Austria, Belgium, Denmark, Finland, Germany, Italy, Sweden, Switzerland, United Kingdom, together with the Joint Research Centre of the Commission of the European Communities. Jointly, organisations from these countries have tackled a range of problems concerned with the improvement and reliability of steam turbines.

One of the coordination groups studied features involved in the fields of stress corrosion and corrosion fatigue attack which are very important considerations for rotating components in the low pressure cylinders of a steam turbine. They also characterised a newly developed steel and considered its suitability for use as steam turbine blades in this part of the machine.

The work of this group is examined in the light of present day literature and experience in this critical review which was conducted with financial assistance from the Commission of the European Communities. The interests of the Management Committee of COST 501 and the wider European industrial situation were represented during the study by a "Steering Group" comprising Dr. S. Ragazzoni, ENEL, Milan, I and Dr. P. Greenfield, GEC Alstom, Leicester, UK.

J. B. Marriott
Secretariat, COST 505

JBM/jb/5/0828
Petten, 5th June 1990



CONTENTS

PREFACE	III
1. Introduction	1
2. Chemical compositions of the steels investigated	1
3. Stress corrosion cracking and corrosion fatigue	2
4. Stress corrosion crack initiation	2
4.1 Corrosion pits, micro-cracks and macro-cracks	3
4.2 Constant extension rate testing, CERT	4
5. Stress corrosion crack propagation	5
5.1 Effects of steel composition on SCC growth rates	7
5.2 Effect of mechanical properties on SCC growth rates	7
6. Stress corrosion crack branching	8
7. Corrosion fatigue crack initiation	9
7.1 Corrosion fatigue crack initiation in LP rotor steels	9
7.2 Corrosion fatigue crack initiation in blading materials	11
8. Fatigue and corrosion fatigue crack growth	11
9. A fracture mechanics analysis of crack initiation	12
10. Considerations concerning the mechanisms of SCC	13
11. Conclusions	17
12. Acknowledgement	19
13. References	19
TABLES	23
FIGURES	25

1. Introduction

Modern steam turbines must retain a very high reliability throughout their service life of typically 200,000 hours. Among the failure modes which have been observed in steam turbines during the last 20 years, stress corrosion cracking was prominent, Ref./1 to 12/. Also, corrosion fatigue has been observed in steam turbine components such as blades and rotors, Ref./13,14/.

It is for these reasons that in the frame of COST program 505, "Materials for Steam Turbines", research projects have been undertaken to study stress corrosion and corrosion fatigue cracking of rotor and blading materials. These projects (see Table 1) have been carried out and coordinated under Group 1 of COST 505. The present paper summarizes the results of this international cooperative research program and, therefore, is essentially based on the final reports, Ref./15 through 27/. Together with additional information from the literature, an attempt is made to describe in quantitative terms the stress corrosion and corrosion fatigue behaviours of steam turbine rotor and blade materials in service-related environments. It is expected that this summary of the results of COST action 505 will be useful for design, operation, development, life time calculations and failure analysis of steam turbines. The paper treats

- stress corrosion crack initiation
- stress corrosion crack propagation
- corrosion fatigue crack initiation
- corrosion fatigue crack propagation

in turn for rotor materials and blade materials.

2. Chemical compositions of the steels investigated

Most of the materials investigated in the program COST 505 are listed in Table 2. This includes the most widely used steam turbine rotor steels, as well as the austenitic-ferritic steel X3CrMnNiMoN 25 6 4 which has recently been developed and modified for steam turbine blading.

The most widely employed steam turbine rotor steel is 26NiCrMoV 14 5, also called 3.5NiCrMoV. Steels No. 1 and 9 in Table 2 are of this variety and were investigated by most participants of COST 505. A number of high purity versions of this steel were also included in the joint research programs (steels No. 2 and 3 in Table 2). A second type of LP rotor steel, 23CrNiMo747, is also widely used and this as well as its high purity versions have also been tested by a number of COST 505 participants (steels 10a, 10b, 11 and 12 in Table 2).

The duplex steel for blades, as well as its low carbon, high tungsten variety appear as number 13 and 14 in Table 2.

3. Stress corrosion cracking and corrosion fatigue

Stress corrosion cracking (SCC) is the initiation and growth of cracks in solids under the simultaneous effects of an aggressive environment and constant or increasing tensile stresses. Corrosion fatigue (CF) is the initiation and growth of cracks under the simultaneous effects of an aggressive environment and cyclic stresses. SCC and CF can be considered as two extremes of a continuous spectrum of different load wave shapes as indicated in Fig. 1. Thus, SCC and CF are two aspects of environment assisted cracking (EAC). In actual steam turbine operation there will always be some cyclic loads on both the rotor and the blades. It is thus sometimes difficult to decide whether a particular failure is by stress corrosion cracking or corrosion fatigue. The important question is then which failure mode is predominant. In many cases this is decided from the fracture appearance, since SCC is predominantly intergranular, along the grain boundaries /10/, while corrosion fatigue is predominantly transgranular across the grains and shows striations and arrest marks /13/. However exceptions from this simplified description are known.

4. Stress corrosion crack initiation

It is easy to say that all stress corrosion service failures and stress corrosion laboratory tests include a time for crack initiation and a time for crack growth. It is more difficult to find out where initiation dominates and where crack growth is of primary importance. In service, this may depend not only on material, stress, and environment, but also on the component size. For example, a stress corrosion crack in service in a steam turbine rotor will sustain a much longer growth time before failure than a stress corrosion crack in a steam turbine blade.

In the laboratory, two types of studies are often carried out to study crack initiation. One type are electrochemical studies, in order to observe the possible reactions of a specific corrosion system, the corrosion rate and mass transfer kinetics, the development and breakdown of surface films, the growth kinetics of local attack and so on. A second type of study deals directly with stress corrosion tests of relatively small specimens where the overall time to failure is probably dominated by the time to crack initiation. Two such stress corrosion tests are widely used with originally smooth specimens: constant stress or constant strain tests, hereafter called time-to-failure tests (TTF) and constant extension rate (CERT)

tests. These methods and their results concerning stress corrosion crack initiation will be discussed in turn.

4.1 Corrosion pits, micro-cracks and macro-cracks

In order to simulate a typical low pressure turbine operating environment, SCC tests were carried out in pure low oxygen condensing steam at 95°C /26,28/. The result is summarized in Fig. 2. The process of stress corrosion crack initiation in 3.5NiCrMoV steels exposed to a steam turbine environment comprises a number of stages. The first is the nucleation and development of localised pitting attack typically, but not exclusively, at the sites of surface breaking non-metallic inclusions.

This is followed by the formation of micro-cracking at the base of certain pits, after an incubation period but still at an early stage of component/specimen life (Fig.2). Micro-cracks do not nucleate at all pits, and their occurrence appears to be critically dependent on the electrochemical nature of the locally contained environment and on stress concentration characteristics. In 3.5NiCrMoV steels, micro-cracking tends to be mainly associated with those pits originating at surface-breaking MnS particles. The relation between the MnS inclusions in the steel and the microcracks observed in stressed specimens is illustrated in Fig. 3.

Typical micro-crack sizes are 0.1 to 0.2 mm. Finally the micro-cracks so formed may become effectively non-propagating or alternatively extend, either as single cracks or more usually by a defect interaction mechanism to a size responsible for failure. Stress corrosion crack initiation was defined as the observation of a macro-crack with a surface breaking length of about 1 mm.

Factors affecting the specific behaviour may be the inclusion characteristics, the strength level of the steel, the applied stress, and the chemistry of the bulk environment /26/. In the COST 505 framework, crack initiation studies have been concentrated on steels of the type 26NiCrMoV14 5, Table 2. Concerning the inclusion characteristics, there is evidence to support the view that the stress corrosion crack initiation resistance of super clean 3.5NiCrMoV may prove to be superior to that of conventional rotor steels due to the lower density of inclusions and the virtual elimination of MnS containing particles in this class of steel /28/. Concerning the effect of applied stress on crack initiation, Fig.2 appears to be substantiated by results from more than one laboratory. The main data base comes from Ref./26/ and /28/. In conjunction with Fig.4 it can be characterized as follows: for condensing steam at 95°C, prepared from deionized feedwater with an oxygen concentration of 7 ppb and a total conductivity of 0.1 μ S/cm, 3.5NiCrMoV steels will develop micro-cracks between 2000 and 5000 hours. Macro-cracks and failures, with smooth tensile specimens and stresses at yield strength level are typically observed after several thou-

sand hours, /12,24,26,31/ if pitting is also occurring. Crack initiation in condensing steam in service has been observed at 50 to 70 percent of the yield strength, emanating from corrosion pits /2,30/. In the laboratory, crack nuclei were found at even lower stress levels, down to 20 percent of yield, but generally, reducing the stress level reduces the probability of crack nucleation and increases the time to crack initiation /26,28/.

A very aggressive environment such as concentrated NaOH (which, in rare cases covers whole turbine rotors and their blades) may cause stress corrosion cracking within hours at high stress levels (Fig.5). Such environments should therefore be avoided in service, particularly since huge stress corrosion service failures have actually occurred with NaOH in steam turbines.

The stress dependence of the time to failure, which is apparent in Figures 5 and 6, has lead to another method to prevent stress corrosion crack initiation in steam turbine rotors. This method uses the introduction of compressive stresses in the surface of the shrunk-on rotor discs. The residual compressive stresses are introduced in at least three additive ways: by proper quenching during heat treatment, by shot peening of the surfaces and by rolling of the keyway holes /8,12,19/. A typical result is shown in Fig.7. Note that ground specimens from COST program D3 /12/ show similar times to failure to the specimens from COST program S1 /24/, demonstrating a much improved stress corrosion resistance under the same conditions /12/.

4.2 Constant extension rate testing, CERT

Slow strain rate stress corrosion testing, otherwise known as constant extension rate testing, may have some advantages over time-to-failure testing and over crack growth rate testing. Such advantages include short testing times and the assurance that there will always be a crack as a result of the testing.

In the present round of COST 505 the CERT test results have not been able to contribute a lot to the understanding or to the prevention of stress corrosion cracking in steam turbines. Not all of the confusion arising from CERT testing may be attributed to this testing method itself. For example, it is stated "CERT tests in de-oxygenated 9M NaOH solution indicate the susceptibility of 3.5NiCrMoV steels to stress corrosion cracking but are not sensitive enough to resolve the relative effect of varying residual element concentrations and the degree of embrittlement", Ref./26/. However it appears from crack growth tests, Ref. /17/ that there is indeed no measurable effect of residual elements and temper embrittlement on SCC of steam turbine rotor steels.

Generalized possible results from CERT-SCC tests are shown schematically in Figure 8. Actually observed data points are presented in Figure 9. It is apparent that slow strain rates down to $1.5 \times 10^{-7} \text{s}^{-1}$ can induce stress corrosion cracking in steam turbine rotor steels in carbonate/bicarbonate solutions at an applied potential of -675 mV (SCE) , and cracking occurs only after the onset of necking in the specimens. No meaningful differentiation of six various experimental rotor steels was thereby possible, Ref./27/.

Further slow strain rate SCC tests with typical steam turbine rotor steels exposed to pure water at 160°C have been carried out with different O_2 and CO_2 contents, Ref./25/. The results are shown in Figures 10 and 11. They confirm that the SCC part of the fracture surface is small but intergranular at low oxygen levels; at high oxygen contents the SCC area is large but transgranular. The CO_2 addition increases the portion of IGSCC. A tendency to transgranular mode in oxygen-containing media was reported also by other authors.

The plastic deformation processes during the CER tests may change the features of SCC and make the data transfer to realistic loading conditions difficult.

5. Stress corrosion crack propagation

It is the purpose of this section to report quantitative stress corrosion crack growth data from steam turbines, and to single out the major influential parameters on the crack growth rates. This chapter summarizes the results of comprehensive comparative studies concerning the stress corrosion crack growth behaviour of steam turbine rotor steels of different chemical composition, purity, and mechanical properties in hot water. The twelve steels of Table 2 were tested with respect to their stress corrosion cracking resistance in water. This large group of steels includes both the typical steam turbine rotor steels /1,8,9,10/ and a number of clean or specially alloyed steels.

The stress corrosion cracking resistance of the steels was investigated by applying fracture mechanics test techniques. Stress corrosion crack growth rates have been measured on pre-cracked specimens of the double cantilever beam (DCB) or compact tension (CT) type which were provided with a fatigue precrack. Knowing the specimen geometry and the crack length, a well-defined stress intensity K_I was applied at the crack tip. This has been done by either using a loading frame where the load P is applied with bolts through holes in the specimen or by inserting a wedge into the notch, which results in a certain deflection δ . In both cases the applied stress intensity can be

calculated from either the applied load P or the deflection δ . The appropriate equations are given in Ref. /10/.

The majority of the stress corrosion crack growth rate measurements reported in this work have been performed on 10 mm thick DCB specimens. About two-thirds of the specimens were wedge loaded; the rest of the specimens were tested under constant load, /7,10,17/.

The results of a large number of stress corrosion crack growth tests in steam turbine rotor steels exposed to 160°C water are shown in Figure 12. Each data point represents the crack growth rate measured in a precracked specimen which had been loaded to a certain stress intensity and then exposed to 160°C water. There is a threshold value of the stress intensity, K_{ISCC} , below which no crack growth could be observed. This threshold stress intensity was found to be between 10 and 20 $MNm^{-3/2}$, Fig.13.

At stress intensities exceeding K_{ISCC} , the cracks extend at a constant growth velocity independent of the applied stress intensity. This is true in particular for very high applied intensities, up to the vicinity of the critical stress intensity K_{IC} , the fracture toughness. Between the lower limit K_{ISCC} (no crack growth at all is observed below this threshold) and the upper limit, a higher stress intensity does not result in an acceleration of the cracks, /10/. This is indicated by the horizontal scatterband of the crack growth curve in Figure 12. The test results show this plateau region for all steam turbine rotor steels tested in their commercially used heat-treatment condition, as demonstrated in Figure 12 where each data point is identified by its corresponding steel number according to Table 2. The observation of a stress-independent crack velocity is of importance for the results below concerning the environmental and metallurgical effects. They have all been measured at stress intensities between 40 and 80 $MNm^{-3/2}$ and thus well within the horizontal part of the crack growth curve.

Temperature and dissolved gases in the hot water could possibly have significant effects on the velocity of stress corrosion cracks. These influences have been investigated in detail and the results are illustrated in Figures 14 to 17. From Figures 14 and 15 the strong temperature effect can be seen. The concentration of dissolved oxygen and carbon dioxide, however, within the limits investigated here, does not have any influence on the stress corrosion crack velocity, as clearly demonstrated in Figures 16 and 17. Thus, for the test results reported below, it is important that the temperature is carefully controlled and the effects of metallurgical variables are compared only at a constant temperature. In the present work this is done primarily at a temperature of 160°C and occasionally, in addition, at 100°C, /10/.

If temperature and yield strength are very similar, then similar stress corrosion crack growth rates are observed by different investigators and different laboratories. This has already been demonstrated in Figures 15, 16 and 17 and it is apparent again in Figure 18, where the main data base is from Ref. /17/, but data from Ref./23/, /27/, /and /31/ agree very well, regardless of oxygen or carbon dioxide concentration.

5.1 Effects of steel composition on SCC growth rates

Figures 19 to 24 illustrate that within the limits of the alloy compositions listed in Table 2, there is no measurable effect of the concentration of phosphorous, manganese, silicon, molybdenum, nickel and sulphur on the growth rate of stress corrosion cracks in low alloy steels when exposed to hot water. Not all of these elements were studied in a controlled way, i.e. changing the concentration of one element while all others were held constant. Nevertheless, according to Table 2, there is a number of steels which are directly comparable with respect to their chemical composition except for one element (for example, number 3 and 4, number 6 and 7, numbers 11 and 12, etc.). Thus, possible synergistic effects of alloying elements appear to be ruled out by this direct comparison. For the turbine rotor steels, it is fair to say that neither the cleanliness nor the base composition of the low alloy steels used for steam turbine rotors has any significant influence on the growth of stress corrosion cracks in these steels when exposed to hot water.

Furthermore, the series of Figures 19 to 24 illustrates again how well the crack growth rate data from Ref. /23,27,31/ agree with the main data base from Ref. /10/ and /17/.

5.2 Effect of mechanical properties on SCC growth rates

Three mechanical characteristics of the steam turbine rotor steels have been studied with respect to their influence on the stress corrosion crack growth rates: fracture toughness, temper embrittlement and yield strength. The results of these investigations are shown in Figures 25 to 28.

The fracture toughness of the steels can be varied in at least three different ways, namely by the sulphur content, by temper embrittlement and by heat treatment, i.e. yield strength. For the present investigation, the first two ways have resulted in fracture toughness values ranging from 110 to 268 MNm^{-3/2}. The different sulphur contents of these steels investigated lead to room temperature fracture toughness values from 196 MNm^{-3/2} up to 268 MNm^{-3/2}. As to temper embrittlement, a commercial ro-

tor steel (number 9 in Table 2) was available in three embrittlement conditions. One was the "as-received" condition, with a fracture toughness of $200 \text{ MNm}^{-3/2}$ measured at room temperature. The other was "as received and step cooled", a heat treatment which resulted in a fracture toughness of $197 \text{ MNm}^{-3/2}$. The third condition simulated a long time operation within the critical temperature interval by tempering the steel at 450°C for 10^4 hours. The resulting room temperature fracture toughness was $110 \text{ MNm}^{-3/2}$. Specimens in all three conditions were supplied as part of the cooperation with COST 505 partner D5.

Figure 25 illustrates the effect of fracture toughness on the stress corrosion crack growth rates. It appears that within the range investigated, the fracture toughness has no influence on the growth rates of stress corrosion cracks as long as the yield strength levels do not differ considerably. This corresponds to the experimental results from Figure 24 which show that the bulk sulphur content does not affect the stress corrosion crack growth rates. Temper embrittlement itself does not influence the growth rates of stress corrosion cracks in hot water, as shown in Figure 26. Note that the plateau stress corrosion crack velocities are very nearly the same regardless of the degree of temper embrittlement. This finding is closely related to Figure 19 which demonstrates that phosphorous segregated to the grain boundaries has no effect on the crack growth rates.

Yield strength however has a pronounced impact on stress corrosion crack growth rates in steam turbine rotor steels. This is illustrated in Figures 27 and 28 where the stress corrosion crack growth rates of rotor steels with different yield strength levels are plotted versus stress intensity and versus yield strength. According to Figure 28 the effect of yield strength on the growth rates of stress corrosion cracks depends on the absolute level of the yield strength. At all testing temperatures, there is a moderate increase of the crack growth rates for yield strengths between 600 and 1000 MPa, and a steep increase of the crack growth rate once the yield strength exceeds 1000 MPa. Both clean and commercial steels exhibit the same yield strength dependence. Similar conclusions have been reached in Ref./31/.

An extensive discussion of these experimental results including a comparison with results from other laboratories is presented in Ref./10/.

6. Stress corrosion crack branching

The great majority of steam turbine rotor stress corrosion service failures are due to intergranular cracking along the grain boundaries, /10/. Such cracks are always branched on a microscopic scale. More interesting is the observation that such service failures also exhibit crack branching on a macroscopic

scale, that is at least two crack branches which grow independently over many grain diameters. Such macroscopic crack branching reduces the stress intensity at each branch compared to a system with a single crack of the same length. This situation has been analyzed theoretically and experimentally and the results are given in Figures 29 and 30, /33/. Note that the stress intensity at branched crack tips decreases (compared to single cracks) by a factor of $1/\sqrt{n}$ when n crack branches exist, Fig.29. With such a reduced stress intensity, branched cracks may grow deeper before the critical stress intensity (fracture toughness) is reached. Theoretically, the critical crack length of an n -fold branched cracking system can be n times longer than a single crack.

This is probably an upper limit and should not be fully used. Nevertheless, if branched cracks may grow deeper before becoming critical, this means that the residual lifetimes of components containing branched cracks will be longer than the residual lifetimes of the same components containing only one single crack of the same depth, /33/.

These ideas have been verified experimentally on specimens from steam turbine rotors containing branched stress corrosion crack systems, /20/. The observations are illustrated in Fig.31, showing that the stress intensities at branched cracks are indeed reduced when the number n of branches is increased, as would be predicted from theory and experiment, /33/.

7. Corrosion fatigue crack initiation

7.1 Corrosion fatigue crack initiation in LP rotor steels

High cycle fatigue crack initiation results from cyclic stresses below the yield strength of the material. Fatigue cracks initiate at points of maximum local stress and minimum local strength. In inert environments a good correlation between the fatigue strength and the tensile strength can be found. Stress concentrations are caused by the design and manufacturing aspects (including technological influences such as roughness and residual stresses) and by the microstructure of the material. Microstructural inhomogeneities such as slip bands with extrusion / intrusion pairs, grain or twin boundaries, inclusions or segregations can be the initiation sites of fatigue cracks.

Corrosion fatigue must be understood as the degradation of the fatigue strength due to the effect of an environment. This includes both the reduction of fatigue strength when the aggressive medium is present and the reduction due to the surface damage after corrosion attack. In contrast to inert environ-

ments, the time-dependent corrosion processes which are superposed on the pure fatigue loading lead to a pronounced frequency dependence. Another consequence is that an endurance limit of ferritic steels can not be observed under corrosion fatigue conditions. It should be noted that the increase of the nominal stresses due to the reduction of area is usually different in laboratory specimens and in real components.

Fatigue investigations are mostly carried out on push / pull fatigue machines or alternating bending machines in single step tests (constant load amplitude) with the fracture of the specimens as the failure criterion. The test duration is a compromise between technical and economical demands and is usual limited to about 10^7 to 10^8 cycles.

Due to the large number of parameters influencing the corrosion fatigue behaviour, it is difficult to compare the results of investigations which were not performed under exactly the same conditions. In order to examine the environmental effect, the reported data concerning the LP steels are normalized and the ratios of the fatigue strength levels in corrosion medium and in air are considered. As it can be seen from Figure 32, which presents the data of the COST programs /16,17/, the reduction of the strength level in deaerated pure water up to 160°C is about 25% of the endurance limit in air at room temperature. In the case of oxygen saturation a much larger effect was observed although no severe surface attack occurred. In both cases we are concerned with a passive corrosion system, but the higher content of oxidation agent obviously results in an earlier nucleation of fatigue cracks at the local sites of film rupture. Slip bands which penetrate the passive layer are such sites of film-free (and therefore unprotected) metal and will be more strongly attacked if the oxidation potential is high. In contrast to oxygenated water the breakdown potential in aerated water is lowered due to the effect of pH reduction (caused by the CO_2 and by atmospheric pollution) and so the level of fatigue strength is additionally reduced by the stress concentrations at the pits and flaws. The same fatigue strength as in aerated water was measured if the surface damage was produced in a precorrosion step and the tests were carried out in oxygenated water. This demonstrates that the difference between aerated and oxygenated water is caused by the mechanical notch effect.

In order to investigate the pure mechanical effect of different forms of corrosion attack, precorroded specimens were fatigued in air and related to the fatigue strength of virgin specimens (Figure 33). It can be seen that pure deaerated water does not produce any surface damage which leads to a reduction of the fatigue strength. After exposure in an acid environment, which led to homogeneous corrosion, the fatigue strength level is lowered by about 20%. In the case of local corrosion, the reduc-

tion depends on the depth and the shape of the pits and flaws and lies between 30 and 65% /16,36/.

With the reported CF data a Smith diagram, normalized with the strength level of the material, is estimated in Figure 34. In addition to the fatigue behaviour in air two limit cases are drawn, representing good and poor service conditions. In pure deaerated water the reduction of fatigue strength is relatively moderate and must be seen as the minimum loss under optimum water chemistry in the turbine. If the service conditions lead to local attack the fatigue strength is reduced drastically. Once initiated, the negative effect of the pits can only be partly removed by better environmental conditions.

7.2 Corrosion fatigue crack initiation in blading materials

Corrosion fatigue is the dominant cause of failure of LP blades. In some cases the corrosion resistance of the conventionally used 12% Cr-steels is not sufficiently high. This gave rise to the activity to develop the ferritic-austenitic steel X2CrMnNiMoN2664 in COST 505 A1. The electrochemical investigations showed a much higher pitting resistance of this steel compared to the 12% Cr steel. This excellent corrosion behaviour can be found also in corrosion fatigue tests. Figure 35 shows Smith diagrams of the X3CrMnNiMoN2664 and a 12% chromium steel X20Cr13 with comparable strength levels, measured under similar conditions. Although in both cases pits are the nucleation sites of the cracks the fatigue strength level of the duplex steel is much higher. Even larger differences can be expected in environments where the 12% Cr steels suffer pitting corrosion but the duplex steel does not.

8. Fatigue and corrosion fatigue crack growth

The series of Figures 36,37 and 38 illustrates the effect of stress intensity, corrosion fatigue and stress corrosion on the growth rates of fatigue cracks. The experimental observations with steam turbine rotor steels, presented in Figure 39 indicate that we have to consider two effects.

The environmental effect significantly increases the propagation rates in the Paris range of the da/dN versus ΔK curves (range of linear relationship in the log-log plot) but influences the threshold values only slightly. Investigations concerning the influence of frequency, temperature and alkalinity substantiated that rotor steels behave according to the "true" corrosion fatigue model of Figure 37.

At low ΔK levels a strong influence of the applied load ratio R on the threshold values ΔK_0 arises. This is because long cracks exhibit the well known closure effect which fakes an unreasonab-

ly high ΔK_0 threshold. Considering these details, one can draw the following conclusion from the work upon which Figure 39 is based, /16,37/:

For the consideration of short defects, such as corrosion pits, the threshold of the closure-free region (high R ratio) should be applied regardless of the effective mean stress. This ΔK_0 value was found to be about 2 MPa \sqrt{m} .

9. A fracture mechanics analysis of crack initiation

It is well known from the literature /38/ and from the authors' own experience, and it has been confirmed again by the cooperative research evaluated here, that fatigue crack initiation can occur readily at small corrosion pits of about 100 micrometers in depth. Moreover, it has been shown that stress corrosion cracks in steam turbine steels also nucleate from corrosion pits, usually 100 to 200 micrometers deep, /12,24,26, 31,34/ and Figures 2,3,4. Thus, it appears meaningful to look at the kinetics of corrosion pit growth, as illustrated in the Figure 40. Clearly pits can grow to 0.1 or 0.2 mm depth in several hundred to several thousand hours. This time is negligible compared to the expected lifetime of steam turbine rotors and blades. Thus, either pitting corrosion in turbines must be reliably prevented or lifetime calculations of components must be based on the growth kinetics of cracks growing out of pits. Pitting attack may be present even on the surfaces of LP discs and rotors which have been run in very carefully operated turbine units. On visual inspection after many thousands of hours of service, such forgings can appear to be in almost pristine condition with only lightly oxidised surface. Nevertheless even in these circumstances, careful metallographic sections can reveal evidence of pits which are not detected by the unaided eye. These may be no deeper than 50 μm , but it has been shown that SCC microcracks can initiate from pits which are only 20 μm deep, if the local encapsulated environment is sufficiently potent /26,28/.

Crack nucleation from corrosion pits can be treated quantitatively by applying concepts from linear elastic fracture mechanics, provided that validity requirements similar to those for sharp cracks are satisfied. In fatigue, these requirements appear to be satisfied for pits 70 μm and more in depth, /38/. In Figure 41, the corrosion fatigue strength, the corrosion fatigue crack growth threshold stress intensity and the results from microscopic pitting studies are linked by the fracture mechanics concept. Note for example from Figure 34 that at an R value of zero the corrosion fatigue strength under pitting condition is 80 ± 80 MPa and thus, the cyclic stress range is 160 MPa. This value is used to draw a horizontal line in Figure 41.

Furthermore, based on Figure 39, a corrosion fatigue threshold stress intensity of about $\Delta K = 2 \text{ MPa}\sqrt{\text{m}}$ is established, depending on the exact definition of that threshold (We may take it to correspond to ΔK which gives crack growth rates of 10^{-11} or 5×10^{-11} meters per load cycle). This threshold $\Delta K = 2 \text{ MPa}\sqrt{\text{m}}$ is shown as a diagonal line in Figure 41. The lines 160 MPa and $2 \text{ MPa}\sqrt{\text{m}}$ intersect at a point which corresponds to $a = 10^{-4} \text{ m}$. This means that whenever pits develop into crack-like shapes of about 0.1 mm depth, the fatigue threshold stress intensity is exceeded at a cyclic stress range of 160 MPa. This is the reason for the low corrosion fatigue strength which is manifest in Figures 32 to 34. It is also the reason for the similarity of the corrosion fatigue strength of steam turbine rotor and steam turbine blade materials under pitting conditions.

Figure 41 permits also a quantitative evaluation of stress corrosion crack nucleation from corrosion pits. Note for example in Figure 13 that stress corrosion threshold stress intensities of steels exposed to water are generally between 10 and 20 $\text{MPa}\sqrt{\text{m}}$. The lower bound value of $K = 10 \text{ MPa}\sqrt{\text{m}}$ has been used to draw a diagonal line in Figure 41. Above it stress corrosion cracking might occur. This line intersects the 800 MPa line (representing typical yield strengths of steam turbine rotor steels) at a point corresponding again to 10^{-4} m . One may conclude from this that steam turbine rotor steel under stresses near the yield strength and exposed to hot water can develop stress corrosion cracks once crack-like pits reach a depth of 100 micrometers. This is in agreement with all the pitting and stress corrosion studies carried out in the cooperative COST 505 research program. Naturally these values are only approximations. If, for example pits would reach a depth of 400 micrometers then, according to Figure 41, stress corrosion cracks could start growing even if the applied stress were only 400 MPa, i. e. half the yield strength.

10. Considerations concerning the mechanisms of SCC

Based on the COST 505 work, in this section an attempt is made to understand the chemical mechanisms of stress corrosion cracking. The driving force for every corrosion process is the thermodynamic instability of the metal in a given environment. If the reactions, which lead to more stable products, are blocked (for example by a protecting film) the system will exhibit local corrosion as soon as the barrier is destroyed locally. In this case in addition to the material and the environment a third component of the corrosion system becomes more important: the mechanical loading.

Before considering the COST 505 results the corrosion system: low alloyed steel / water, i.e. iron / water should be described briefly:

At surfaces of low alloyed steels exposed to pure neutral or weakly alkaline water, hydroxide or oxide films develop. Initially an amorphous $\text{Fe}(\text{OH})_2$ film grows, which converts afterwards to magnetite (Fe_3O_4) according to the Schikorr reaction. The velocity of this reaction is very low at ambient temperature; above 100 °C its rate is noticeable and above 230 °C spontaneous formation of magnetite takes place /41,42/. In acid environments the iron goes into solution as the Fe^{2+} ion and in strongly alkaline media the complex ion FeO_2H^- is formed.

The cathodic reaction in pure water is always the development of hydrogen from protons if no oxygen or other oxidizing agents are present.

Local forms of corrosion appear when the breakdown potential of the passive films is exceeded. This breakdown potential is mainly influenced by the kind and concentration of film destroying ions (such as chlorides), by the temperature and the pH value /43/.

It is well known that the stress concentration caused by pits can reduce the fatigue strength level of a material drastically. The COST 505 work on SCC initiation has focussed interest on the nucleation and growth of pits also as a prior step to stress corrosion cracks.

Pits, micro- and macro-cracks were found in specimens exposed to condensing pure steam. These results shall be considered together with other investigations in order to come to a consistent model.

In /16/ measurements in a closed autoclave system were carried out. Although the conductivity increased considerably during the tests no indications of growing pits were found. Similar results are reported after long term exposure /31/; neither in deaerated nor in oxygenated water was localized attack observed. This means that water as a bulk environment is much less aggressive than condensing steam although its content of impurities might be higher than those of the feed water of the steam cycle.

It is well known that the content of impurities in the first condensate can be much higher than in the steam, depending on the distribution coefficient of the agent. However the results of /31/ showed that a high content of impurity is not absolutely necessary to understand crack nucleation.

Typical intergranular SCC appeared if the environments were not refreshed or if crevice conditions were applied, i.e. if stagnated conditions were present. Obviously condensate films are comparable to those stagnating environments.

Under stagnating conditions the requirements are given for the development of concentration elements at an inhomogeneous metal surface (surface-breaking inclusions, inhomogeneous passive

film, mechanical defects or crevices with the possibility of the development of ventilation elements) and so for the appearance of stable anodic and cathodic zones. Due to hydrolysis of the corrosion products the aggressivity of the local environment at the anodic zones may increase whereas the cathodic regions are inhibited by an increase in pH value at the wall.

The pit depth increases according to a logarithmic time law; i.e. the growth rate decreases because a saturation of the pit electrolyte with metal ions takes place and the mass transfer is hindered more strongly if the diffusion distances to the bulk solution are larger. The shape of the pits, which is usually more or less hemispherical, can change if tensile stresses are present. In /26/ it was observed that certain pits showed higher growth rates at the tip of the pit than at the side walls; this means the shape of such pits tends to become crack-like. The density of these "high activity pits" increases with the applied stress. The stress concentration at the pit tip seems to activate this zone whereas the side walls repassivate. The final stage of this process is the development of micro-cracks at the activated pit tip. A necessary assumption for the formation of crack is that the growth rate of the pit is not higher than that of the crack. Obviously the transition takes place if the current densities at the pit tip and the tip of the intergranular SCC crack are of the same order.

The experimental findings of crack initiation at anodic zones point to an anodic mechanism of crack growth. The fact, that the SCC rate is less influenced by the composition of the bulk solution, by the load level and the crack geometry (diffusion distances) indicate the development of a local corrosion system. This system is characterised by a local crack tip environment which repassivates the crack flanks immediately after crack propagation.

The SCC propagation in high-strength material is often explained by a hydrogen mechanism. Atomic hydrogen, which is developed by the cathodic partial reaction of the corrosion, can be absorbed by the metal lattice. It diffuses to so-called hydrogen traps (grain boundaries, dislocations or other defects of the lattice structure) and embrittles the material. Although investigations are still necessary to clarify the mechanism in detail some remarks can be made:

Of course the plastic zone in front of the crack tip, with its microstructural defects, is a highly active hydrogen trap, and the energy to crack an embrittled material is lower. However the model of pure hydrogen induced cracking (HISCC) seems not to be applicable. This becomes evident in the inhibition of SCC propagation after cathodic polarisation /44,45/. According to the classical model of HISCC, cracking is caused by the activity

of hydrogen in the lattice regardless of where the hydrogen comes from, i.e. it is independent of an anodic reaction. The embrittlement by hydrogen of LP rotor steel should be seen as an "alloying effect" which changes the properties of the material and which has a crack accelerating effect. It is not held for the causal reason of crack propagation in dilute aqueous environments (even for high strength materials).

From the result that pitting and SCC can appear in pure low oxygen steam at relatively low load levels one could conclude that all rotors exhibit SCC microcracks. Since the microcracks and the pits, at which these cracks are initiated, are too small for a visual inspection or for non-destructive test methods this conclusion can hardly be verified. However the development of macrocracks, which were found in the experiments after some tens of thousands of hours at high load levels, does not agree with the experiences in many stations. Therefore in the following some ideas concerning possible differences between the laboratory and the service environments shall be outlined:

- In the laboratory tests the conductivity of the feedwater for the steam generation was carefully controlled and held at a low level. The conductivity is a general measure for the sum of all ion impurities contained in the water; the aggressivity of the condensate phase however depends on the kind and the distribution coefficient of these impurities. Additionally non-ion agents, which are not measured by a conductometer, can produce aggressive environments in the steam cycle. This means that we cannot exclude different effects of media with the same low conductivities.
- Specific impurities in the steam cycle of a power plant can be deposited in the dry part of the HP and IP and hence be missing from the LP environment (specially if a closed loop is installed).
In the laboratory tests the steam is condensed directly in the specimen chamber and then discarded. The effect mentioned above is not possible.
- Steam in power plants is doped with alkalisation agents. An increased pH in the condensate shifts the pitting potential to higher values and makes the occurrence of pits less probable.
- The velocity of steam flow is much higher in the turbine than in the test rig. This may decrease the possibility of the development of concentration elements at the steel surface (thinner condensate films; more turbulent flow with better exchange between steam and condensate phase).

- The position of the first condensate depends on the operating conditions. Locally established corrosion systems can be dried out or washed away.

In order to minimise local forms of corrosion in LP rotors all actions which increase the difference between the breakdown potential and the open circuit potential and which eliminate stagnating environments are welcome.

- Due to a low content of impurities in the feedwater the danger of the enrichment of the film-destroying agents in the condensate decreases and results in a higher breakdown potential.
The measurement of the conductivity is a simple and robust method to monitor the impurity level. Since a low conductivity alone is no guarantee for a low aggressivity further analyses and sporadic inspections during standstills are necessary to ensure a sufficient steam quality.
- The reliable alkalisation of the condensate film increases the breakdown potential. It should be remarked that the pH of the first condensate phase can be quite different from the pH of the bulk condensate.
- The open circuit potential is based on the equilibrium of the anodic and cathodic reactions and so on the kind and concentration of oxidizing agents. Oxygen is present in the LP turbine only during a trip, not during normal operation. If no other oxidizing impurity is present the open circuit potential is dependent on the H_3O^+ / H_2 - reaction, i. e. on the pH. The lower the H_3O^+ concentration (= the higher the pH) the lower the open circuit potential.
- During shutdown phases condensing moisture in the presence of air (and the air pollutants) can produce environments of high aggressivity. The turbine should be kept dry during this time.

11. Conclusions

The cooperative research program COST 505 has achieved significant progress in the field of stress corrosion cracking and corrosion fatigue of steam turbine rotor and blade materials.

The central role of pitting as nucleation sites for stress corrosion and corrosion fatigue cracking has been demonstrated. It is therefore clear that the prevention of pit formation is a worthwhile goal, although in practical terms the total elimination of this form of attack may be impossible to achieve. Nevertheless, both stress corrosion and corrosion fatigue crack



initiation processes are statistical events and any steps taken to minimise the incidence of pitting will markedly reduce the probability of these two forms of environmental cracking. The results of the COST 505 collaboration have shown that such measures include the adoption of steels with low volume fractions of non-metallic inclusions, the avoidance of surface residual tensile stresses during the final stage of manufacture, the minimisation of the static and dynamic service stresses, the limitation of the strength levels of the applied materials and the avoidance of crevices and stagnating conditions.

An important contribution can be provided by the water chemistry. The impurities contained in the steam cause either deposits in the dry part of the turbine (with subsequent increase of the steam consumption and possible corrosion during the shut-downs) or an aggressive environment in the first condensate. A correct supervision of the medium purity, consisting of the immediate detection of any contamination and the quick application of corrective actions, can minimise the risk of environmental induced failures.

The aggressivity of the environment in a steam / water loop is hardly predictable because it is dependent on the quality of the chemical supervision, thus on decisions made by the operators. So the quality of the chemical supervision, which determines the medium purity, should be evaluated periodically by a specialist. The inspections should include:

- On-line check of the chemical parameters and of the monitoring equipment
- Inspection of the equipment during overhauls. This observation should check the cleanness of the turbine and the heat exchangers and allow a quantification of any deposits and / or of corrosion in the system.

Since pit formation is often related to sporadic abnormal service conditions and since pits can stop propagation due to a changed environment, a lifetime calculation is not possible in advance. Such calculations are meaningful if cracks have already appeared because their growth kinetic are less influenced by the bulk medium and can be described using fracture mechanics.

Despite the advances in understanding the mechanism of SCC initiation and propagation there are still open questions concerning the environmental conditions required in order to be sure of avoiding pit nucleation. For a more detailed quantitative fracture mechanics analysis, threshold stress intensity measurements and pitting kinetics studies need further refinement.

The development of an austenitic-ferritic blading steel with considerably higher corrosion fatigue resistance than the conventional 12% Cr steel was successfully finished. This material is applicable to blading designs which do not require a yield strength above 600 MPa or the induction hardening of the leading edges.

12. Acknowledgement

This study has been conducted with the financial assistance of the Commission of the European Communities, under contract no. COST -0010-CH (CH).

13. References

- /1/ Kalderon, Proc.Instn.Mech.Engrs., Vol.136, 1972, pp 341-377
Steam Turbine Failure at Hinkley Point A
- /2/ Hodge, Mogford, Proc.Instn.Mech.Engrs., Vol.193, 1979,
pp 93-106, UK Experience of Stress Corrosion Cracking in
Steam Turbine Disks
- /3/ Lindinger, Curran, Materials Performance, Feb.1982, pp 22-26
Experience with Stress Corrosion Cracking in Large Steam
Turbines
- /4/ Lyle, Burghard, Materials Performance, Nov.1982, pp 35-44,
Cracking of Low Pressure Turbine Rotor Discs in US Nuclear
Power Plants
- /5/ Lyle, McMinn, Leverant, Proc.Instn.Mech.Engrs., Vol.199,
1985, pp 59-67, Low pressure steam turbine disc cracking -
an update
- /6/ Czajkowski, Weeks, Materials Performance, March 1983,
pp 21-25, Examination of Cracked Turbine Discs from Nuclear
Power Plants
- /7/ Speidel, Magdowski, Second International Symposium on Envi-
ronmental Degradation of Materials in Nuclear Power Systems
-Water Reactors, Monterey, CA, Sept.9-12, 1985, Stress Cor-
rosion Cracking of Steam Turbine Steels - An Overview
- /8/ Engelke, Schleithoff, Jestrach, Termuehlen, Proc. of the
American Power Conference, Vol.45, 1983, Design, Operating
and Inspection Considerations to Control Stress Corrosion of
LP Turbine Disks
- /9/ Aubry, Duchateau, Technology of Turbine Plant Operating with
Wet Steam, London, 1988, French Experience of Corrosion in
Nuclear Turbines
- /10/ Magdowski, Speidel, Metall.Trans.A., Vol.19A, 1988, pp 1583-
1596, Clean Steels for Steam Turbine Rotors - Their Stress
Corrosion Cracking Resistance
- /11/ Jaffee, Metall. Trans.A.,1986, Vol.17A, pp 755-75
- /12/ Schleithoff, David, Schmitz, Ewald, DVM-Arbeitskreis Bruch-
vorgänge, 1988, pp 167-180, Spannungs-Risskorrosion an Tur-
binenradscheiben

- /13/ Hagn, "Lifetime Prediction for Parts in Corrosive Environments", in Corrosion in Power Generating Equipment, M. O. Speidel and A. Atrens, eds., Plenum Press, N.Y. and London, 1984, pp 481-516
- /14/ "Advances in material technology for fossil plants", Viswanathan and Jaffee, editors, ASM International, 1987
- /15/ COST 505 A1, Final Report, Hochörtler et al, 1989
- /16/ COST 505, CH3, Final Report, Denk, Maggi, Scarlin, 1989
- /17/ COST 505, CH4, Final Report, Magdowski, Speidel, 1988
- /18/ COST 505, D2, Final Report, David, 1988
- /19/ COST 505, D3, Final Report, David, 1988
- /20/ COST 505, D5, Final Report, Berger, 1989
- /21/ COST 505, D6, Final Report, Wunderlich, Schmitt-Thomas, 1989
- /22/ COST 505, D28, Final Report, David, 1988
- /23/ COST 505, I5, Final Report, Pozzi, Gabetta, 1989
- /24/ COST 505, S1, Final Report, Tavast, 1989
- /25/ COST 505, SF3, Final Report, Hietanen, 1989
- /26/ COST 505, UK11, Final Report, Holdsworth, Burnell, 1989
- /27/ COST 505, UK20, Final Report, McIntyre, Mulvihill, Trant, 1989
- /28/ S.R.Holdsworth, G.Burnell and C.Smith, "Factors influencing stress corrosion crack initiation in super clean 3.5NiCrMoV rotor steel". To be published in proceedings of EPRI-conference on clean steels, Japan, 1989, by ASTM, 1990
- /29/ Oeynhausen et al, "Reliable Disk-Type Rotors for Nuclear Power Plants", American Power Conference, Chicago, April 27-29, 1987
- /30/ B.W. Roberts and P. Greenfield, "Stress Corrosion of Steam Turbine Disc and Rotor Steels", Corrosion, NACE 35, (1979) pp 402-409
- /31/ David, Schleithoff, Schmitz, "Spannungsrissskorrosion in hochreinem Wasser von 3 1/2% NiCrMoV-Vergütungsstählen für Dampfturbinen-Scheiben und -Wellen", Mat.-Wiss.u.Werkstofftechnik, Vol.19, 1988, 43-50 und 95-104
- /32/ Maggi, BBC internal report
- /33/ Ruth M.Magdowski, Peter J.Uggowitzer and Markus O.Speidel, "The effect of crack branching on the residual lifetime of machine components containing stress corrosion cracks", Corrosion Science 25 (1985) pp 745-756
- /34/ Müller, "Theoretical Considerations on Corrosion Fatigue Crack Initiation", Metallurgical Transactions A, Vol.13A, 1982, pp 649-655
- /35/ Schieferstein, Schmitz, "Korrosions-Zeitschwingfestigkeit von Turbinenwerkstoffen unter betriebsähnlichen Beanspruchungen" VGB Kraftwerkstechnik, Vol.58, 1978, pp 193-260
- /36/ T.C.Lindley, P.McIntyre and P.J.Trant, "Fatigue crack initiation at corrosion pits". Metals Technology 9 (1982) pp 135-142
- /37/ M.O.Speidel, ETH Zürich, unpublished work 1982
- /38/ Markus O.Speidel and Andre Pineau, "Fatigue of high-temperature alloys for gas turbines", in High-Temperature Alloys for Gas Turbines, Applied Science Publishers, London, 1978, pp 479-512
- /39/ M.O.Speidel, Corrosion Fatigue in Fe-Ni-Cr Alloys, in "Stress Corrosion Cracking and Hydrogen Embrittlement of Iron Base Alloys", NACE 5, NACE, Houston, TX, 1977, 1071-1094
- /40/ S.Sakurai et al, "Failure analysis and life assessment of low pressure turbine blades", American Power Conference, 1989

- /41/ Härderlius, "Kenntnis der Schutzwirkung und Stabilität von Oxidschichten auf Stahl in alkalischen und neutralem Wasser", Mitteilungen des VGB, April 1966, pp 132-141
- /42/ Potter, "Neue Vorstellungen über die Reaktion zwischen Stahl und Wasser bei hohen Temperaturen", Mitteilungen des VGB, February 1962, pp 19-22
- /43/ Pourbaix, "Significance of Protecting Potential in Pitting and Intergranular Corrosion", Corrosion NACE, Vol.26, 1970, pp 479-500
- /44/ Congleton, Shoji, Parkins, Corrosion Science, Vol. 25, 1984, pp 633-650
- /45/ Shalvey, Corrosion NACE, Vol.39, 1983, pp 66-70

Table 1: Projects of COST 505, Group 1

Project	Lab.	Title	Investigations	Materials	Environments
A1	VEW Kapfenb.	Advanced Materials for the Final Stages of Steam Turbines	Production of test melt. Forging and heat treatment.	X3CrMnNiMoN2564 Duplex Steel	-
CH3	ABB Baden	Failure Mechanisms in Steam Turbine Rotors	CF, da/dN	3.5NiCrMoV 2Cr1Ni, 2Cr2Ni	Pure Water RT - 160 °C (autoclave)
CH4	ETH Zürich	SCC of Steam Turbine Rotor Materials	SCC propagation Fracture mechanics	commercial, clean experimental rotor steels	Pure Water RT - 160 °C (autoclave)
D1	MPI Düsseld.	Effect of P-content on Mechanical Properties and Corrosion Behavior	Auger investigations SCC.	Various	-
D2	Siemens- KWU Mülheim	Corrosion Fatigue of Turbine Rotors under Operating Conditions	CF, Pitting	3.5 NiCrMoV	Condensate (aerated, oxygenated)
D3	Siemens- KWU	Influence of Residual Compressive Stresses on the SCC Behaviour	SCC initiation after surface treatments	3.5NiCrMoV	NaOH/NaCl- solution
D5	Siemens- KWU Mülheim	Crack Growth and Fracture of Stress Corrosion Cracks	ΔK_0 and K_{IC} of branched SCC cracks	3.5NiCrMoV	air
D6	TU München	Corrosion Fatigue of Duplex Steels under Simulated Turbine Conditions	CF, Pitting	X3CrMnNiMoN2564	Chloride solutions, pH3-7 80-150°C
D2B	Siemens- KWU Mülheim	Corrosion Behaviour of the X3CrMnNiMoN2564 under Service Related Conditions	CF, SCC, Pitting	X3CrMnNiMoN2564	Chloride solutions, pH3-7 80°C
I5	CISE Milano	SCC Behaviour of LP Disc and Rotor Materials	SCC propagation Fracture mechanics	3.5NiCrMoV 2Cr1Ni	Pure water
S1	ABB Finspong	SCC initiation Mechanism in Steam Turbine Rotors	SCC initiation	3.5NiCrMoV 2Cr1Ni and other steels	NaOH and aerated water
SF3	VTT Tampere	Stress Corrosion Cracking of LP Rotor Steels	CERT	3.5NiCrMoV 2Cr1Ni	Pure water + O ₂ , CO ₂ (autoclave)
UK11	GEC Rugby	Stress Corrosion of LP Discs and Rotors	SCC initiation	3.5NiCrMoV and embrittled	Pure condens- ing steam 95°C
UK20	CEGB Leatherh	Effect of Pitting and Alloy Content on SCC	Pitting, SCC initiation and propagation, CERT	3.5NiCrMoV experimental steels	Pure condens- ing steam 95°C

Table 2 Chemical compositions of steam turbine rotor and blade steels

steel number	designation	chemical composition, weight-percent												
		C	Mn	P	S	Si	Ni	Cr	Mo	V	Al	Sn	As	Sb
1	26NiCrMoV14 5	0.28	0.19	0.008	0.005	0.18	3.57	1.44	0.40	0.12	n.d.	0.011	sum	0.009
2	"	0.31	0.02	0.0024	<0.001	0.03	3.42	1.44	0.40	0.10	n.d.	0.0032	sum	0.005
3	"	0.26	0.031	0.0012	0.0012	0.022	3.47	1.65	0.45	0.10	0.006	0.003	0.003	0.0009
4	HP + 0.15Mn	0.26	0.15	0.0013	0.0013	0.019	3.51	1.67	0.45	0.10	0.005	0.003	0.003	0.0009
5	HP+Sn+As+Sb	0.26	0.031	0.0012	0.0012	0.021	3.47	1.65	0.45	0.10	0.006	0.011	0.008	0.0013
6	CP + 0.15Mn	0.24	0.17	0.010	0.008	0.012	3.57	1.68	0.44	0.10	0.006	0.010	0.006	0.0016
7	CP + 0.35Mn	0.24	0.37	0.010	0.008	0.014	3.52	1.67	0.44	0.10	0.005	0.010	0.006	0.0014
8	26NiCrMo 12 7	0.20	0.43	0.012	0.009	0.20	3.11	1.72	0.57	0.07	n.d.	0.004	n.d.	n.d.
9	26NiCrMoV14 5	0.30	0.35	0.006	0.006	0.05	3.58	1.65	0.41	0.10	n.d.	0.008	0.015	0.003
10a	23CrNiMo747	0.20	0.52	0.011	0.007	0.23	0.96	1.73	0.56	0.005	n.d.	0.005	n.d.	n.d.
10b	"	0.20	0.62	0.006	0.005	0.18	1.02	1.85	0.55	0.01	0.005	0.010	0.003	0.002
11	"	0.22	0.020	0.002	<0.003	0.015	1.10	1.87	0.60	0.051	0.017	0.007	<0.005	<0.001
12	"	0.23	0.020	0.002	<0.003	0.007	1.10	1.75	0.003	0.044	0.010	0.005	<0.005	<0.001
13	X3CrMnNiMoN 2564	0.036	5.8	0.027	0.002	0.31	3.8	25.3	2.22		W=0.06		N = 0.32	
14	X3CrMnNiMoN 2564	0.020	5.6	0.007	0.002	0.38	3.8	25.8	2.10		W=0.45		N = 0.33	

HP - High purity
 CP - Commercial purity

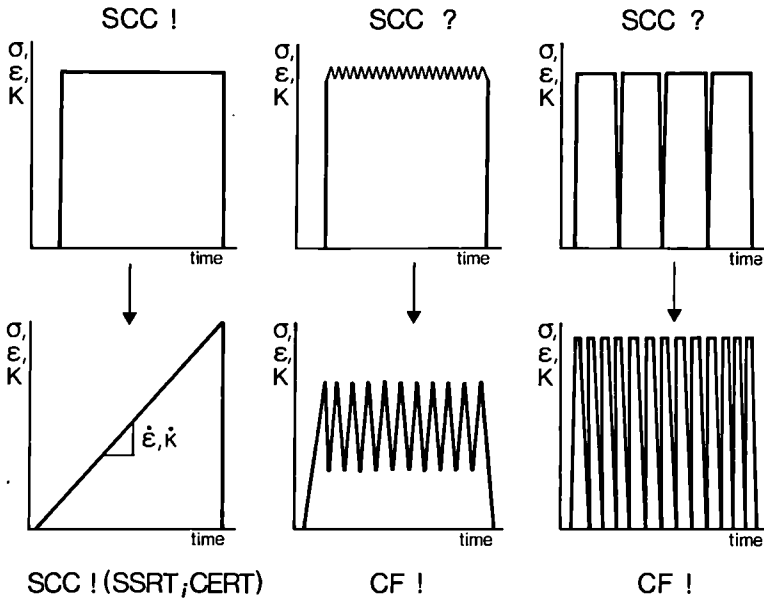


Fig. 1 Transitions between load wave shapes underlying stress corrosion cracking and corrosion fatigue. Stress σ , strain ϵ , or stress intensity K as functions of time. Upper and lower left clearly would cause stress corrosion cracking (SCC). Lower middle and lower right clearly would cause corrosion fatigue (CF). Upper middle and upper right define load wave shapes which could cause either stress corrosion cracking or corrosion fatigue. Elements of the latter load wave shapes are frequently encountered on steam turbine rotors and blades in service.

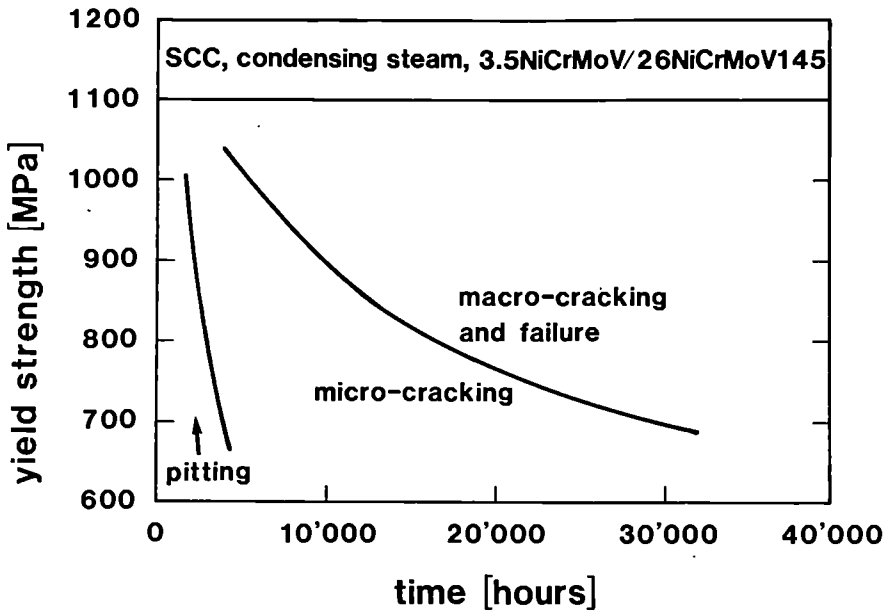


Fig. 2 Steps toward stress corrosion cracking in typical turbine rotor steels in condensing pure steam (95°C) or immersed in stagnating pure water of 80-100°C, and loaded at yield strength level/Ref.26,28/. Typically, as first step stress corrosion cracks start with a high probability from corrosion pits at surface breaking MnS inclusions, then develop into intergranular micro-cracks of several 100 μm. In a second step, micro-cracks grow to the size of about one mm and so become macrocracks. Small specimens may then fail, but large, tough rotors may still have a significant residual lifetime. During the first step, pitting may be minimized by good water chemistry, avoiding crevices and possibly by the use of clean steels with low inclusions content, /Ref.26,28/. During the second step, micro-cracking may be minimized by low applied stresses, or the application of compressive surface stresses (e.g. shot peening),/Ref.19/.

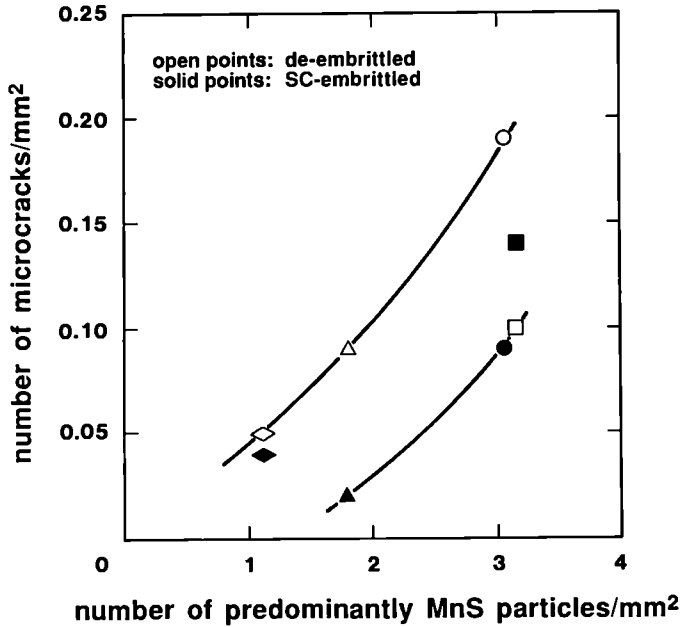


Fig. 3 The relationship between the number of high-activity (i.e. micro-crack-producing) pit sites and predominantly MnS bearing particle area fraction, /26/. Bend specimens of commercial 3.5NiCrMoV steels in the de-embrittled or step-cooled (SC) embrittled condition were loaded to 110 percent of the yield strength for 1200 hours in pure steam at 95½C.

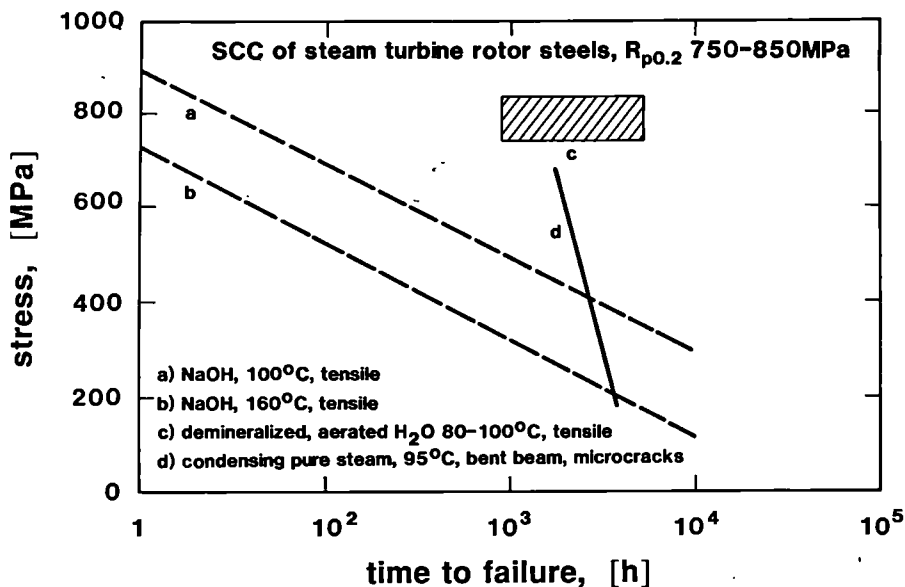


Fig. 4 Effect of stress and environment on time to stress corrosion crack initiation in typical steam turbine rotor steels, /Ref. 12, 24, 26, 31/. Note that in water and condensing steam cracks are observed after several thousand hours if the specimens are stressed near the yield strength and if the environment permits pitting corrosion to develop around MnS-inclusions. After 12000 hours, microcracks are observed at very low stress levels in pure condensing steam. Lines a and b refer to Figures 5 and 6.

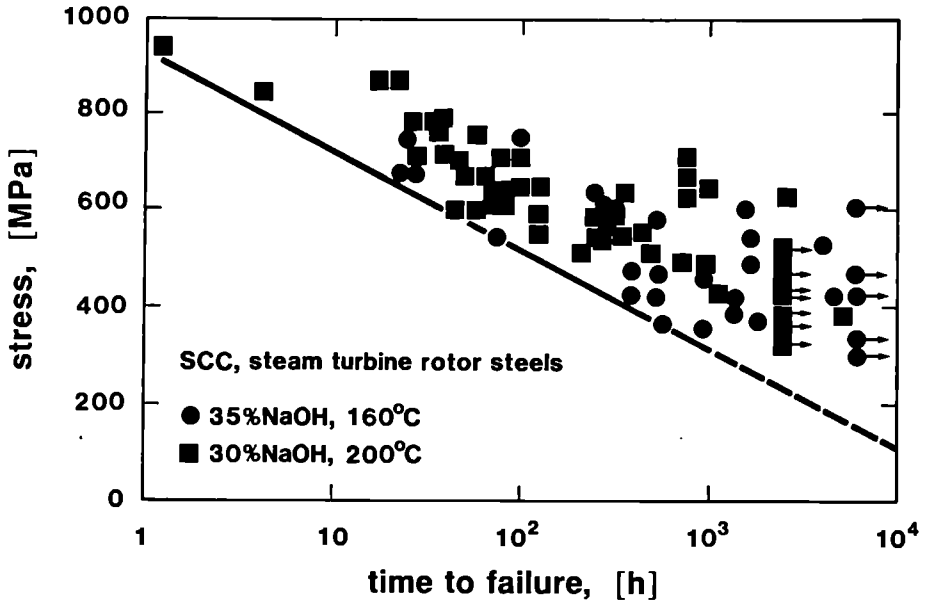


Fig. 5 Stress corrosion cracking of steam turbine rotor steels in concentrated aqueous NaOH solutions. Effect of applied stress on the time to failure of originally smooth thin specimens. Different investigations under slightly different conditions yield similar results /24, 31/.

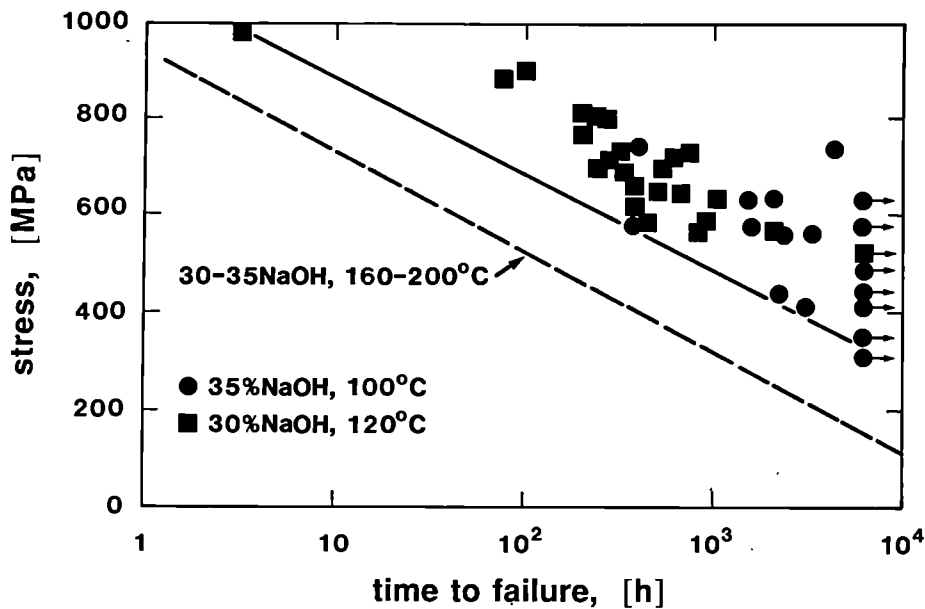


Fig. 6 Lower temperatures result in longer times to failure by stress corrosion cracking compared to the data in Fig. 5, /24, 31/. Note in both, Figures 5 and 6 that the time to failure increases with lower applied stress.

Stress Corrosion Cracking Tests

35% NaOH + 3.5% NaCl at boiling temperature of 123°C
tensile specimen (ϕ 5.5 mm)

○ ground ● shot peened surface, D3

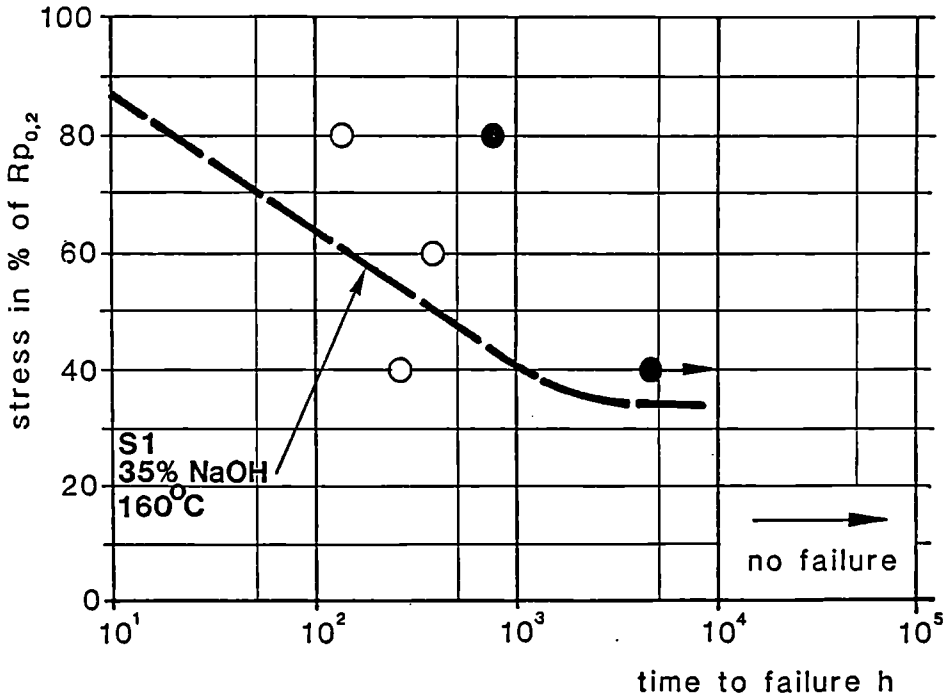


Fig. 7 Stress corrosion specimens from two different COST programs show similar times to failure when tested in hot concentrated NaOH solutions, Ref. /12,24/. Shot peening considerably lengthens the time to failure, Ref. /12/.

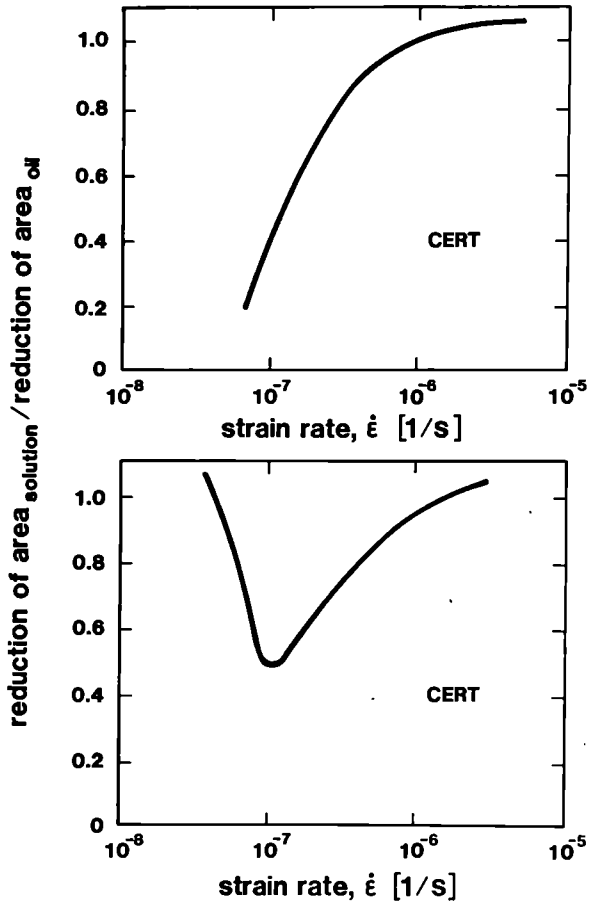


Fig. 8 Schematic representation of two possible effects of strain rate on ductility in CERT - SCC tests.

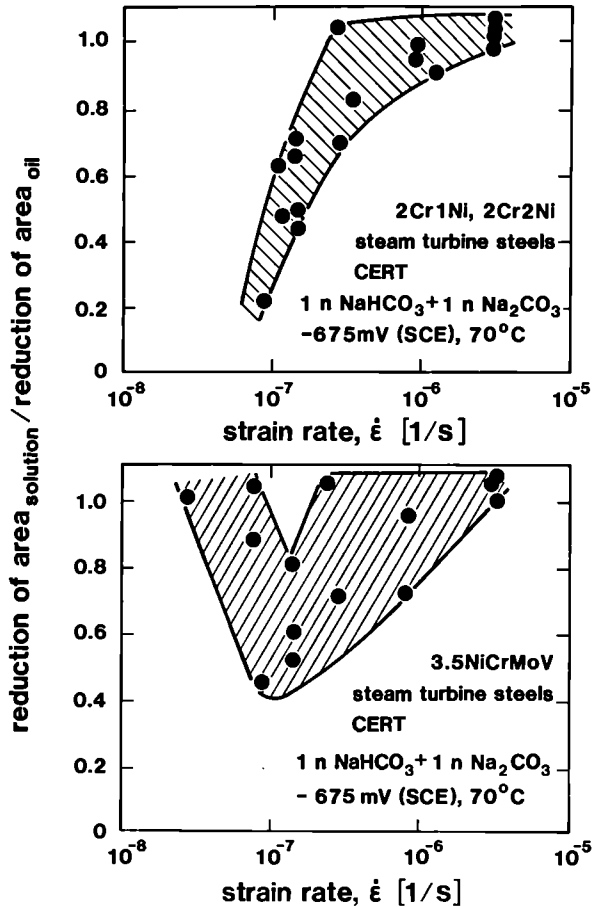


Fig. 9 Both effects shown in Fig. 8 are observed in reality, Ref. /27/, but the meaning and the use of such data is not clear, other than that they demonstrate qualitatively a "low susceptibility to stress corrosion cracking".

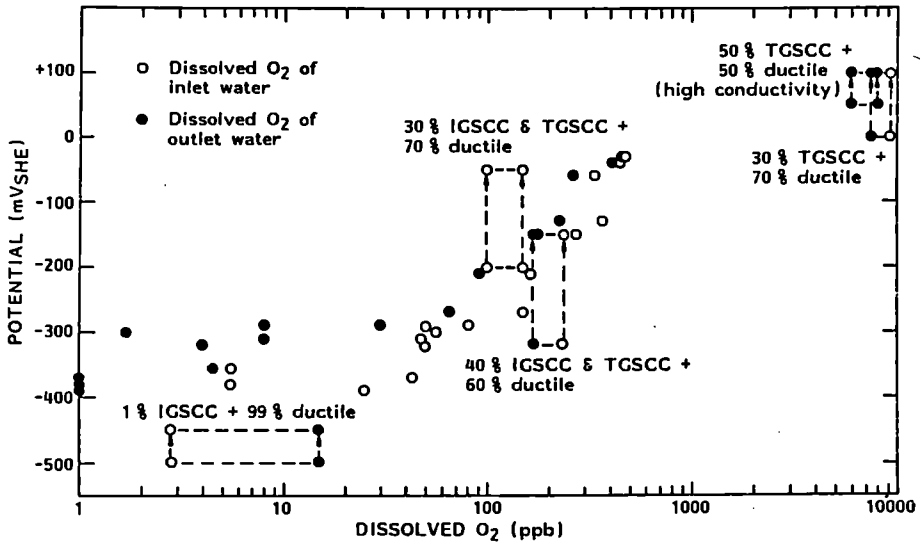


Fig. 10 Effect of dissolved oxygen content on potential and CERT stress corrosion cracking of steam turbine rotor steel (3.5NiCrMoV) in high-purity water at 160°C, Ref./25/.

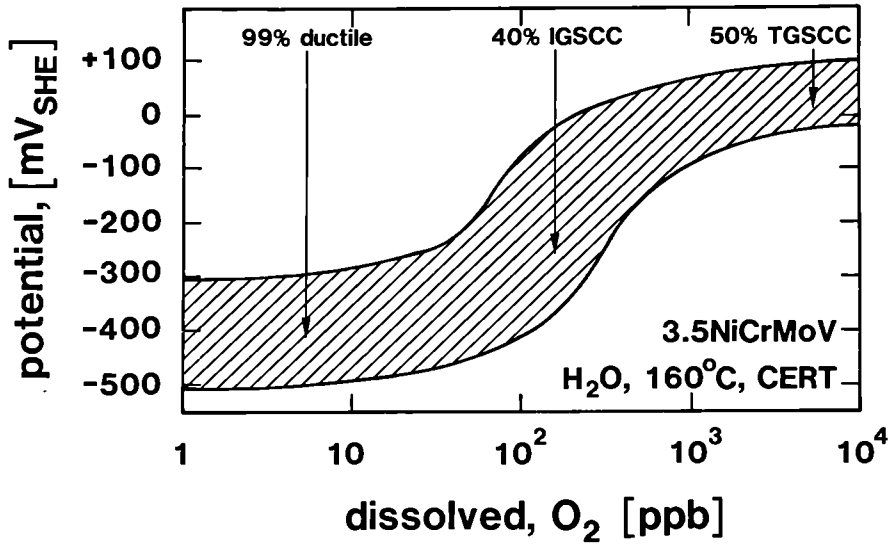


Fig. 11 Schematic evaluation of the results in Fig. 10. Note that only at intermediate oxygen concentrations intergranular SCC has been observed. IGSCC dominated only when CO₂ was also added, Ref. /25/.

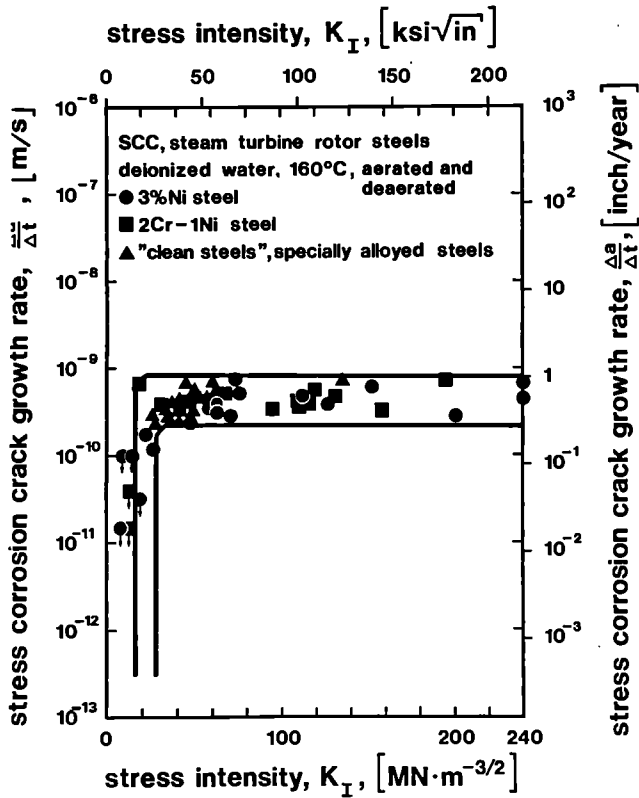


Fig. 12 Effect of stress intensity on the growth rate of stress corrosion cracks in various steam turbine rotor steels, exposed to water at 160°C.

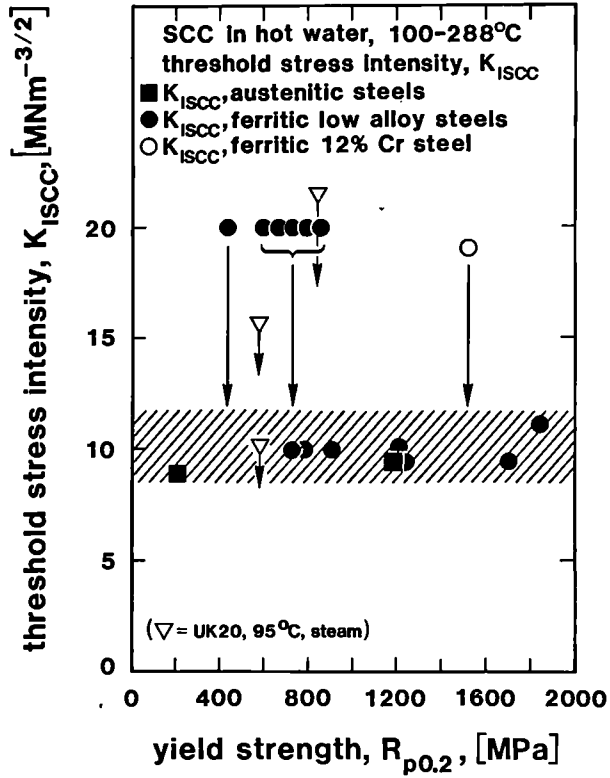


Fig. 13 Stress corrosion threshold stress intensities of various steels in water, Ref. /10, 17, and 27/. Note that K_{ISCC} is between 20 and 10 $MNm^{-3/2}$ ($\approx MPa\sqrt{m}$).

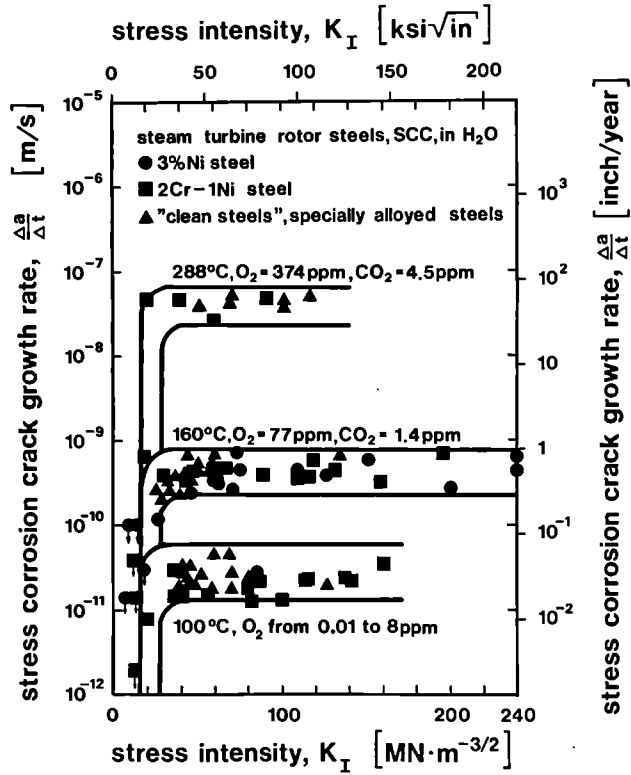


Fig. 14 Effect of temperature and stress intensity on the growth rates of stress corrosion cracks in steam turbine rotor steels, Ref. /10, 17/.

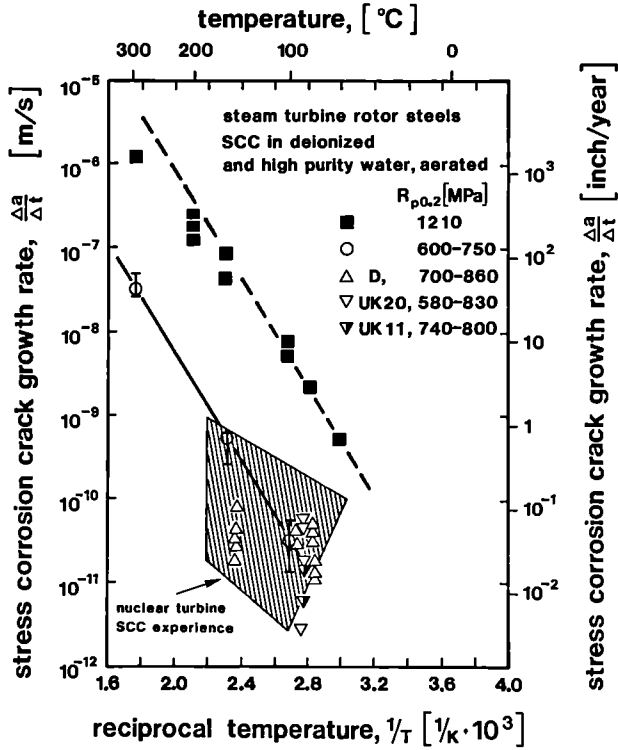


Fig. 15 Effect of temperature on stress corrosion crack growth rates. The shaded area indicates the service experience of steam turbine rotors. Solid points and open circles from Ref. /10/ and /17/. Other experimental data from Ref. /31/ (D), Ref. /27/ (UK20) and Ref. /26/ (UK11).

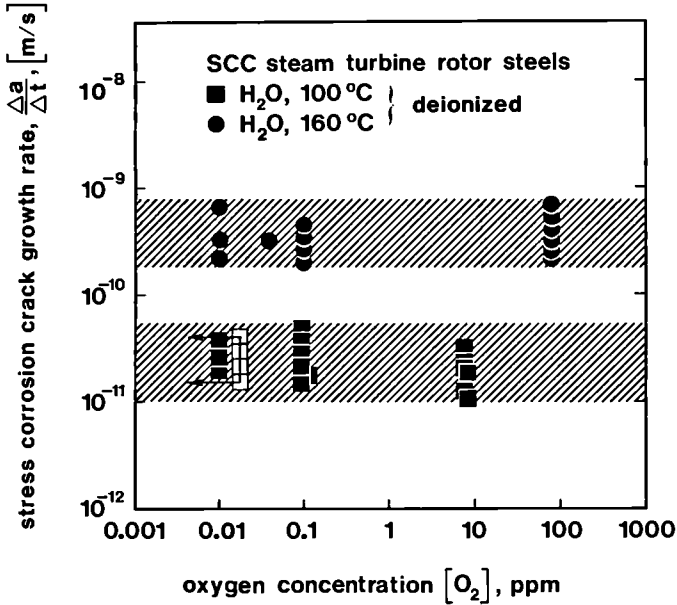


Fig. 16 Effect of dissolved oxygen on stress corrosion crack growth rates in steam turbine rotor steels exposed to water, Ref. /17/. Additional data (open squares) from Ref. /31/. The partly intergranular SCC observed in CERT tests in water with 200 ppb O_2 and 1 ppm CO_2 . Ref. /25/, falls also in the 160°C scatterband shown here (9×10^{-10} m/s).

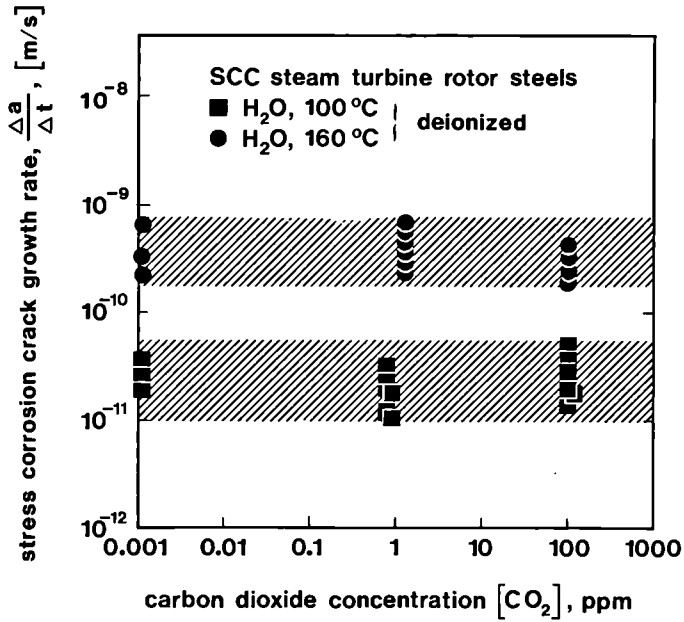


Fig. 17 Effect of carbon dioxide concentration on stress corrosion crack growth rates in steam turbine rotor steels exposed to hot water, Ref. /10, 17/. The partly intergranular SCC crack growth rates observed by CERT in water with 200 ppb O₂ and 1 ppm CO₂, Ref. /25/, fall also in the 160°C scatterband shown here. The crack growth rate data measured in COST Program I5, Ref. /23/, fall also in the 100°C scatterband shown here (3×10^{-11} m/s).

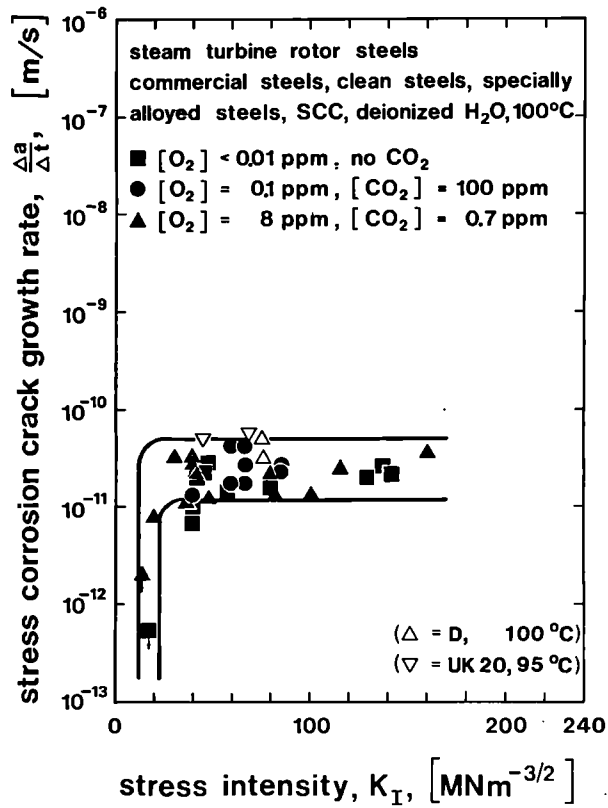


Fig. 18 Effect of stress intensity, oxygen, and carbon dioxide on stress corrosion crack growth rates in steam turbine rotor steels in water near 100°C. Main data base from Ref. /10/ and /17/, but data from Ref. /23/, /27/, /31/ agree very well with it.

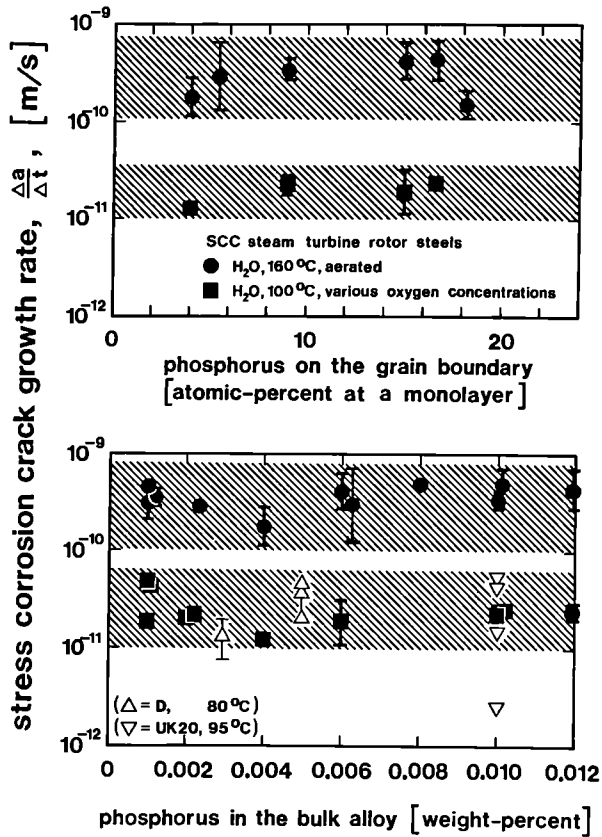


Fig. 19 Neither the phosphorous content in the bulk alloy nor the phosphorous concentration at the grain boundaries have any influence on the growth rate of stress corrosion cracks. Steels according to Table I. The applied stress intensities range between 40 and 80 $\text{MN}\cdot\text{m}^{-3/2}$. Note that data from Ref. /31/ (D) and Ref. /27/ (UK20) agree with the main data base from Ref./10/,/17/

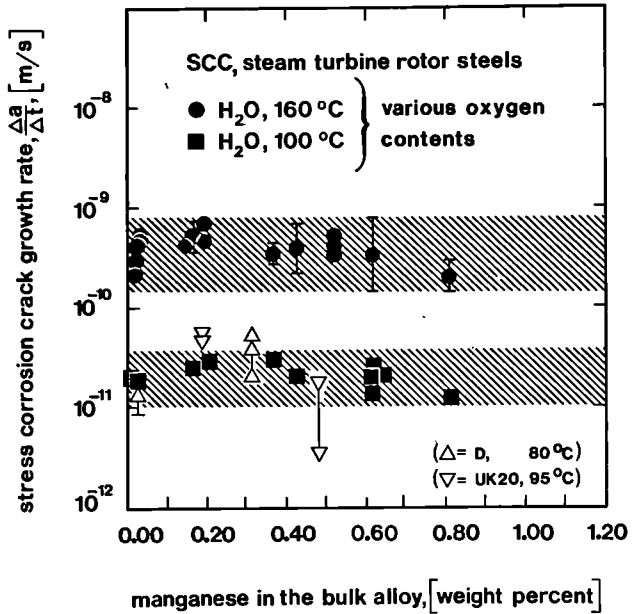


Fig. 20 The manganese content of the steels has no influence on their stress corrosion crack growth rate. Steels according to Table I. The applied stress intensities range between 40 and 80 $\text{MN}\cdot\text{m}^{-3/2}$. Note that data from Ref. /31/ (D) and Ref. /27/ (UK20) agree with the main data base from Ref./10/,/17/.

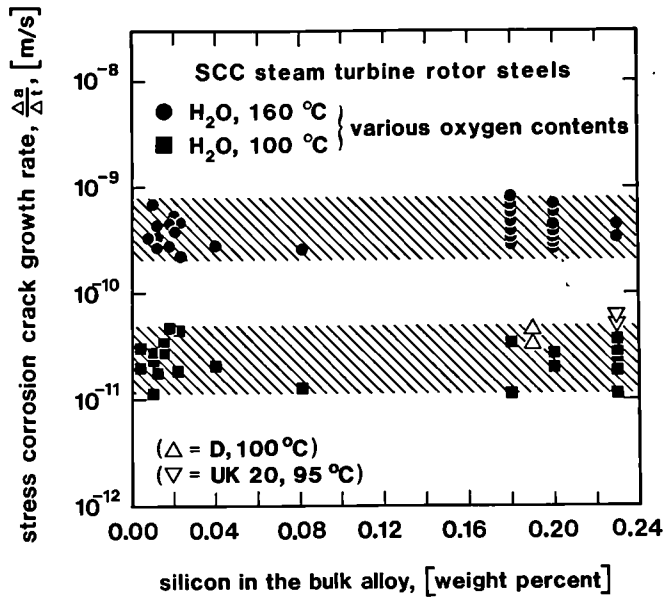


Fig. 21 The silicon content of the steels has no influence on their stress corrosion crack growth rate. Steels according to Table I. The applied stress intensities range between 40 and 80 $\text{MN}\cdot\text{m}^{-3/2}$. Note that data from Ref. /31/ (D) and Ref. /27/ (UK20) agree with the main data base from Ref./10//17/.

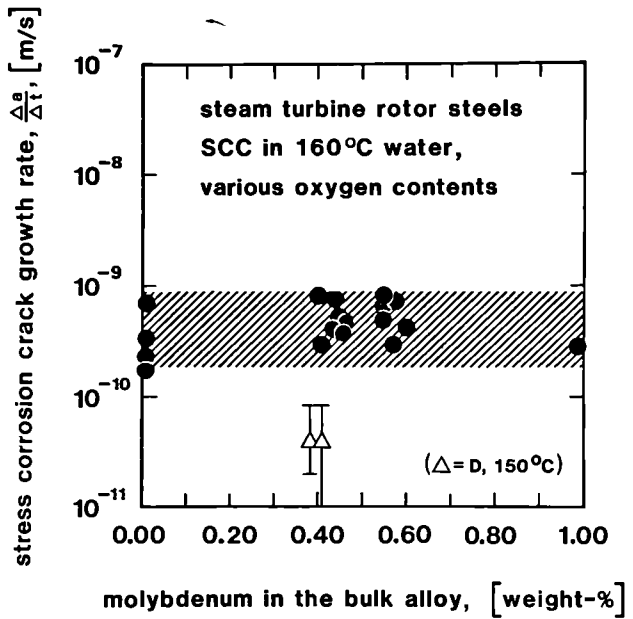


Fig. 22 The molybdenum content of the steel has no influence on their stress corrosion crack growth rate. Steels according to Table I. The applied stress intensities range between 40 and 80 $\text{MN}\cdot\text{m}^{-3/2}$. Data from Ref./10,17/. Note the somewhat lower data from Ref./31/ (D), due partly to lower temperature.

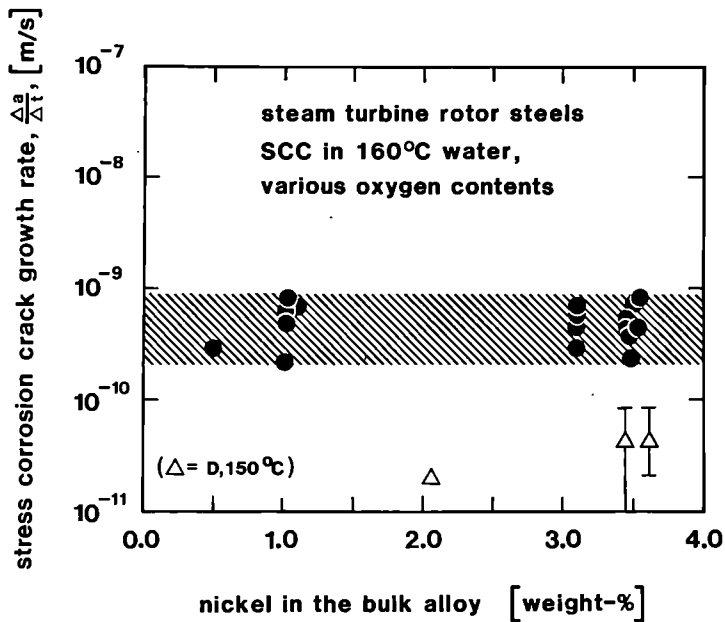


Fig. 23 The nickel content of the steels has no influence on their stress corrosion crack growth rate. Steels according to Table I. The applied stress intensities range between 40 and 80 $\text{MN}\cdot\text{m}^{-3/2}$. Note the somewhat lower data from Ref. /31/ (D), due partly to lower temperature.

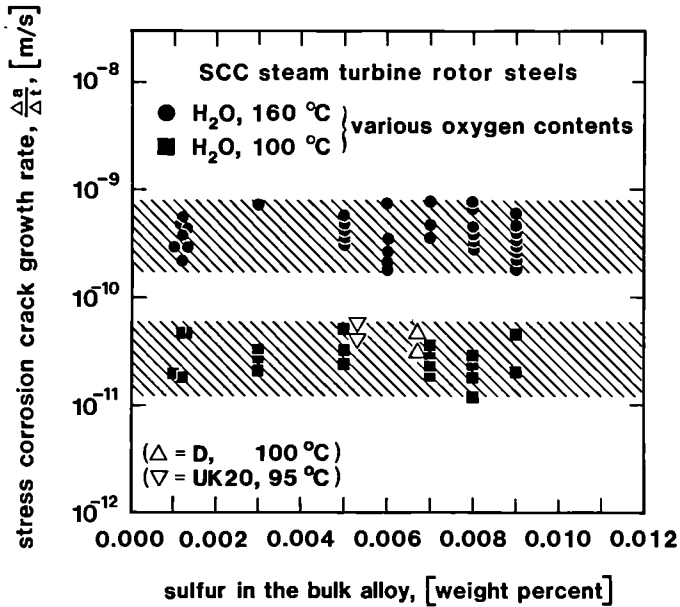


Fig. 24 The sulfur content of the steels has no influence on their stress corrosion crack growth rate. Steels according to Table I. The applied stress intensities range between 40 and 80 $\text{MN}\cdot\text{m}^{-3/2}$. Note that data from Ref. /31/ (D) and Ref. /27/ (UK20) agree with the main data base from Ref./10/,/17/.

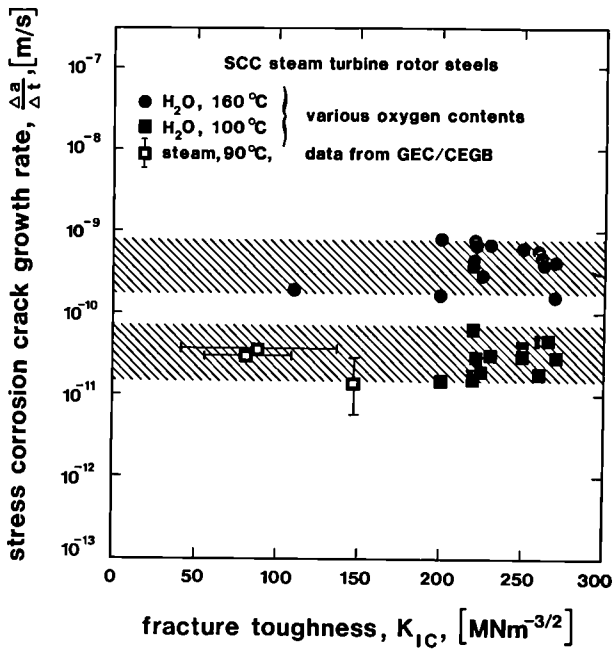


Fig. 25 At comparable strength levels, there is no effect of fracture toughness on the growth rates of stress corrosion cracks. Fracture toughness values taken at room temperature solid points from Ref. /10,17/. GEC/CEGB data from Ref./2/. Steels according to Table I. The applied stress intensities range between 40 and 80 MN·m^{-3/2}.

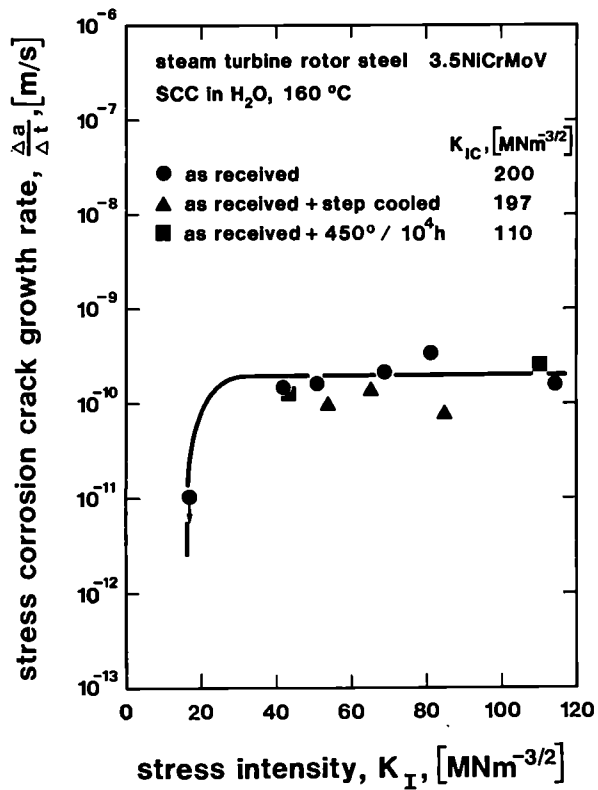


Fig. 26 The stress corrosion crack growth rates in the plateau range appear to be independent of the degree of temper embrittlement. Steel number 9 in Table I. The fracture toughness values are taken at room temperature. Ref./10,17/.

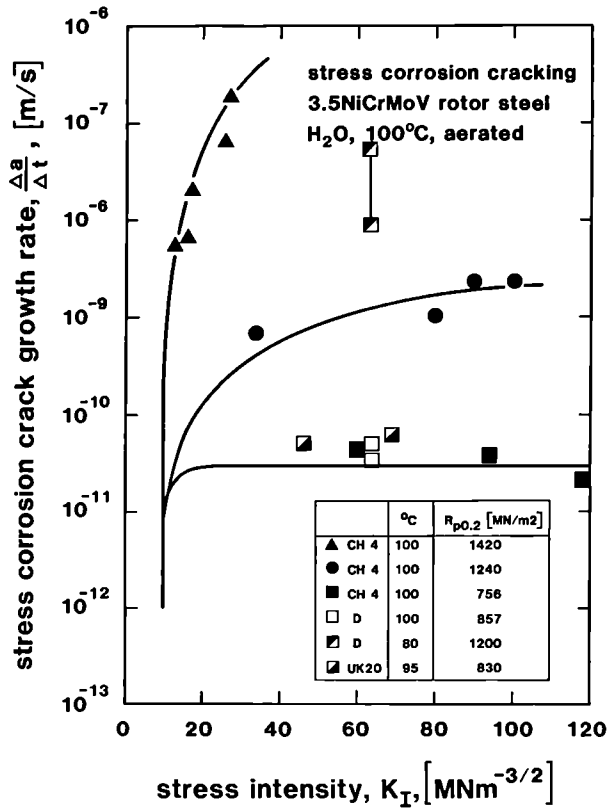


Fig. 27 Effect of stress intensity and yield strength on the growth rates of stress corrosion cracks in steam turbine rotor steel exposed to water near 100°C. Note that data from four different sources coincide closely: Ref. /17/ (CH4), Ref. /31/ (D), Ref. /27/ (UK20) and Ref. /23/ (15, 3×10^{-11} m/s, 100°C, $R_{p0.2} = 670$ MPa).

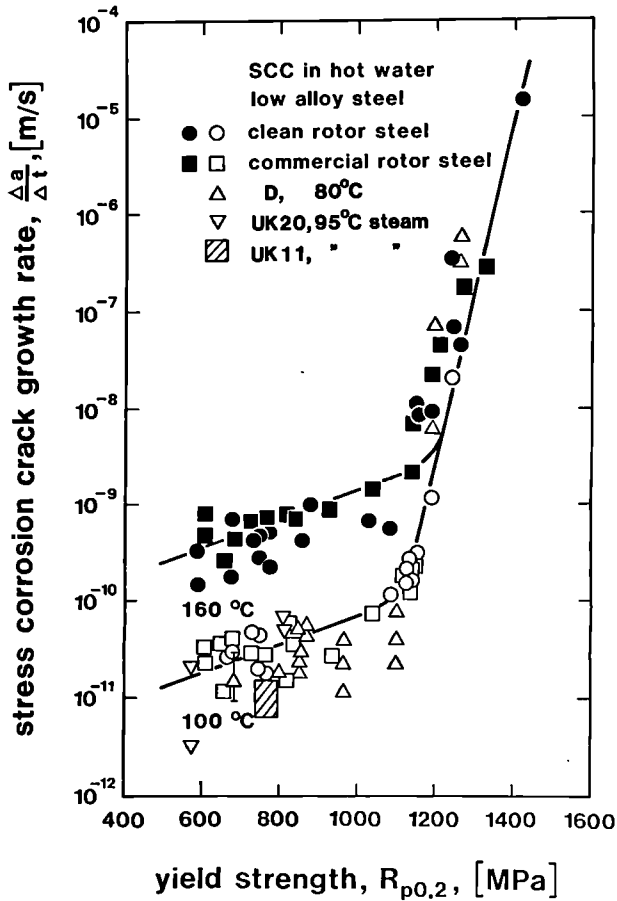


Fig. 28 There are two different effects of yield strength on stress corrosion crack growth rates: A moderate one at low strength levels. Steels according to Table I. The applied stress intensities range between 40 and 80 $\text{MN}\cdot\text{m}^{-3/2}$. There is no difference in the yield strength dependence between clean rotor steels and commercial rotor steels. Main data base from Ref. /10/, /17/. Additional data from Ref. /26/ (UK11), Ref. /27/ (UK20) and Ref. /31/ (D). The very satisfactory agreement between the results from these different sources means that the COST 505 program has now achieved a reliable reference data base.

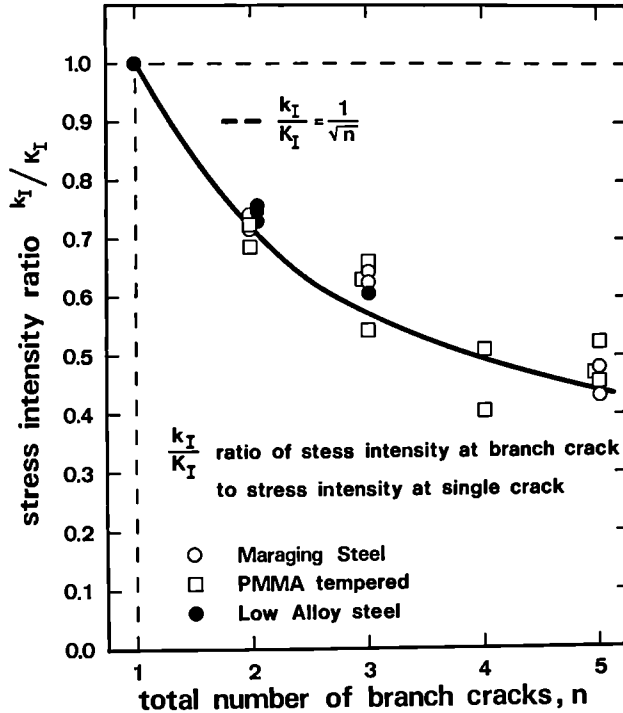
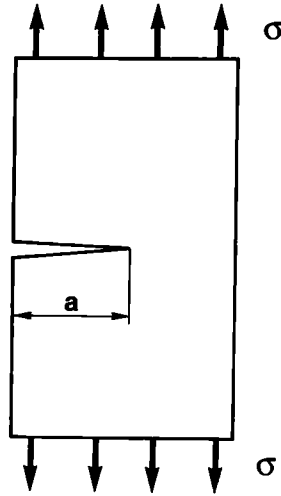


Fig. 29 The stress intensity at branch cracks decreases as the number n of branch cracks increases. This can be experimentally verified by measuring the fracture toughness in materials with branched precracks. Ref. /33/.

critical depths of single and branched cracks

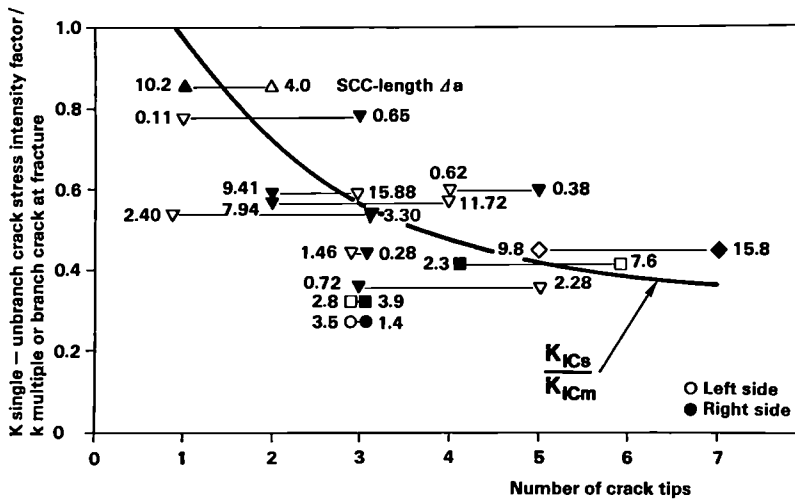


single crack: $K = \sigma \sqrt{a_s} \cdot Y$

crack with n branches } $k = K/\sqrt{n}$
 $k = \sigma \sqrt{a_s/n} \cdot Y$

$a_{cn} = n a_{cs}$

Fig. 30 Since the stress intensity at branched cracks is smaller, the critical depth of such cracks is larger, Ref. /34/. This means longer residual lifetimes of cracked components.



Influence of Number of SCC-Crack Tips on Stress Intensity Factor

Fig. 31 The stress intensity at branch cracks is smaller than at single cracks. Observations on specimens from steam turbine rotors containing actual stress corrosion crack systems, Ref. /20/.

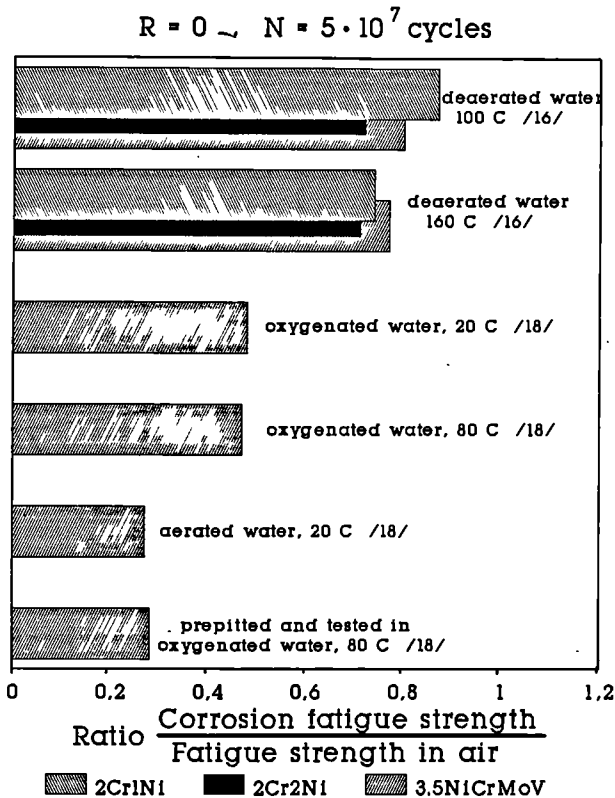


Fig.32 Normalized corrosion fatigue strength of the LP-steels in different environments. In deaerated and oxygenated water no severe corrosion attack was observed. The reduction of fatigue strength can be explained by the microscopic attack of slip bands. In aerated water and pre-pitted specimen additionally the notch effect due to pits takes place.

$R = 0$, $N = 5 \cdot 10^7$ cycles

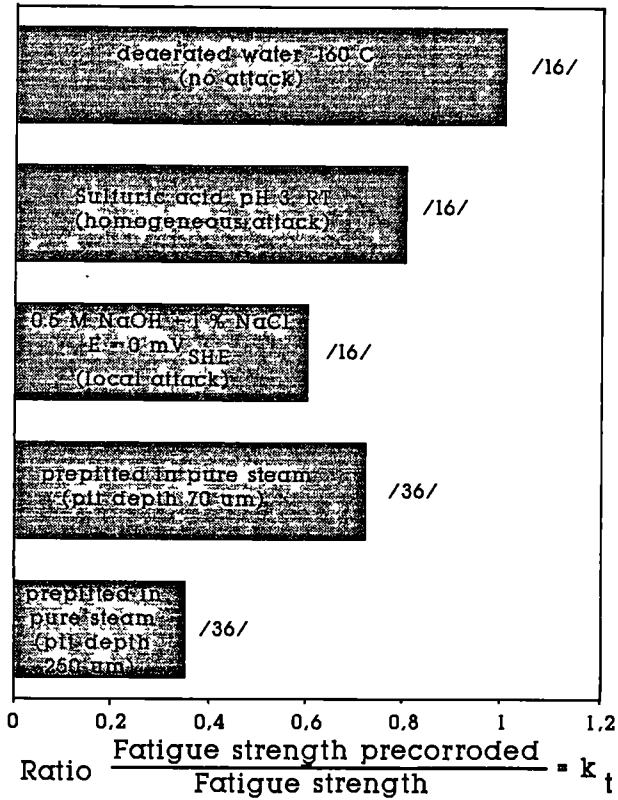


Fig.33 Pure notch effect of precorroded specimens (tested in air after precorrosion)
 Homogeneous attack causes moderate fatigue strength decrease. Strong reduction can appear after local corrosion depending on the size and the geometry of the surface defects.

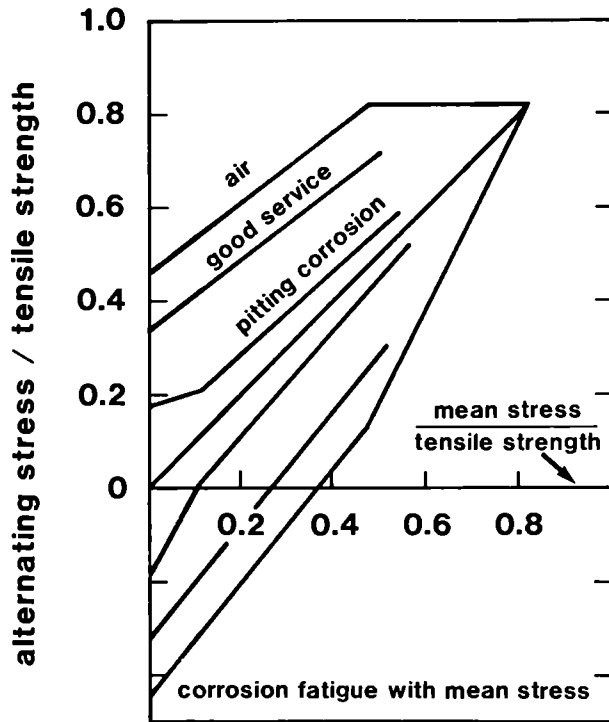


Fig. 34 Schematic representation of the effect of mean stress and environments on the fatigue strength of steam turbine rotor and blade steels. Note that pitting corrosion should be avoided if acceptable fatigue strength is desired.

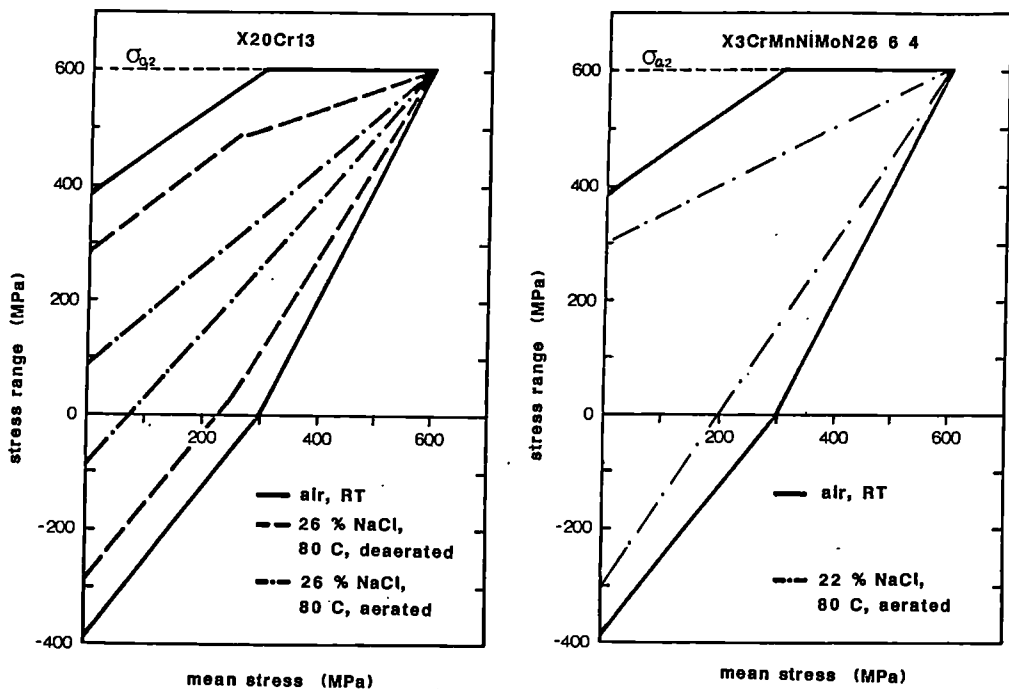


Fig.35 Comparison of the corrosion fatigue behaviour of a conventional 12% Cr-steel and the duplex steel developed in COST 505.

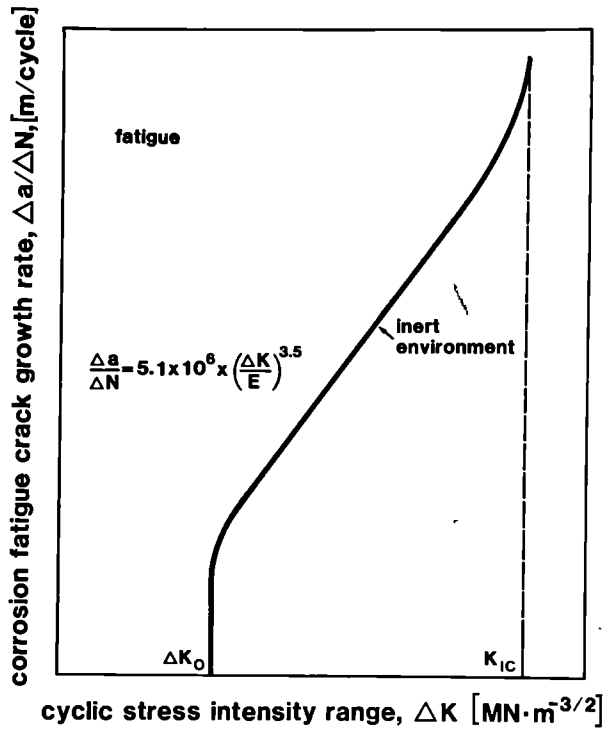


Fig. 36 Schematic representation of the effect of the cyclic stress intensity range on the growth rates of fatigue cracks in metallic materials exposed to inert environments, /35/, /36/.

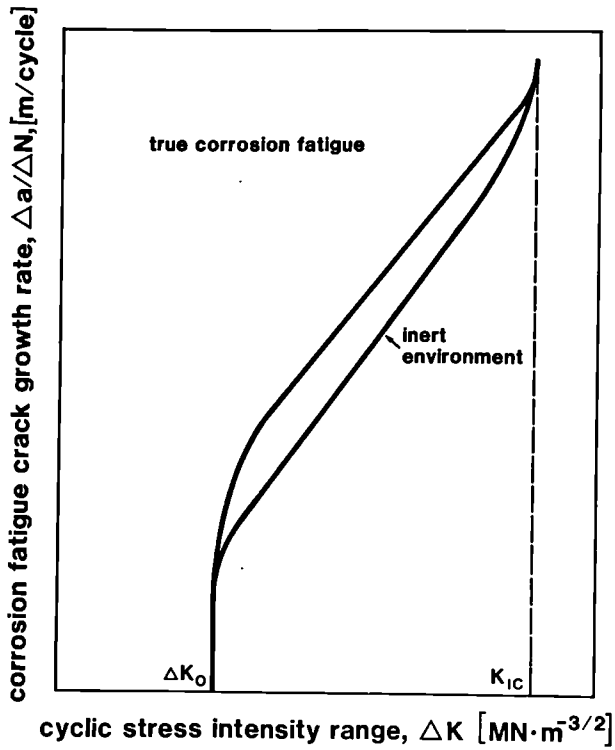


Fig. 37 In "true" corrosion fatigue there is a clear but limited acceleration of the growth rate of fatigue cracks compared to inert environments, /36/.

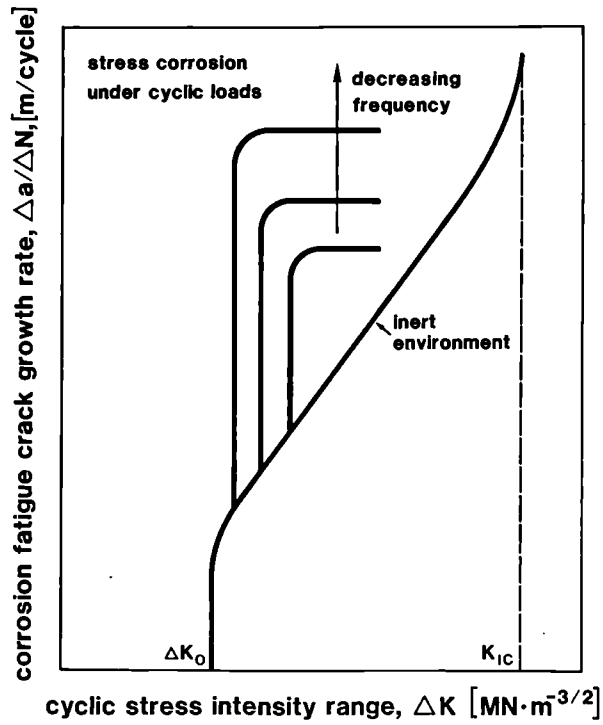


Fig 38 If stress corrosion is possible at the same time as fatigue, crack growth rates per load cycle can become very high and they are also strongly frequency dependent, /36/.

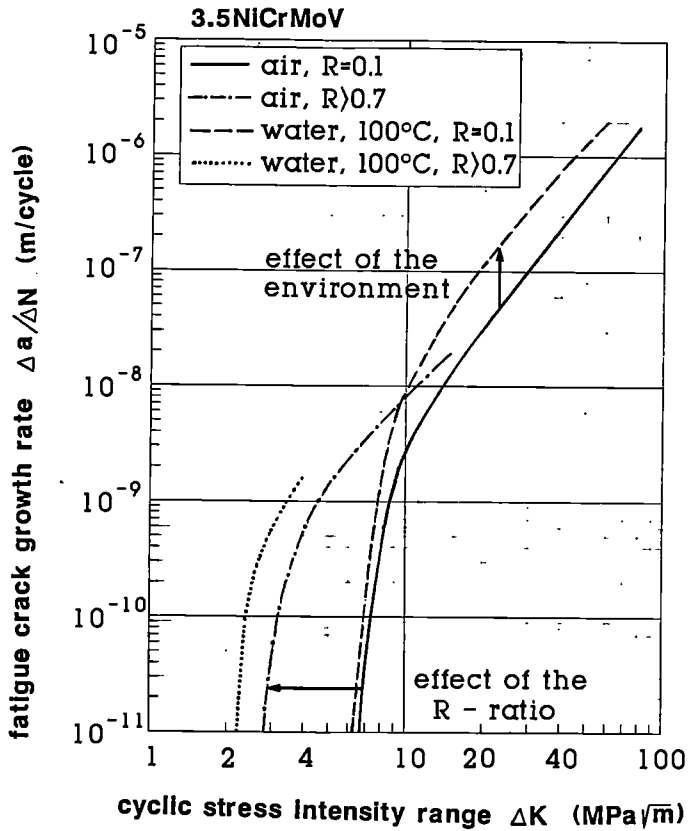


Fig.39 Fatigue and corrosion fatigue crack growth rates observed in the 3.5NiCrMoV steam turbine rotor steels, based on references /16,37/. The curves of other LP steels are very similar.

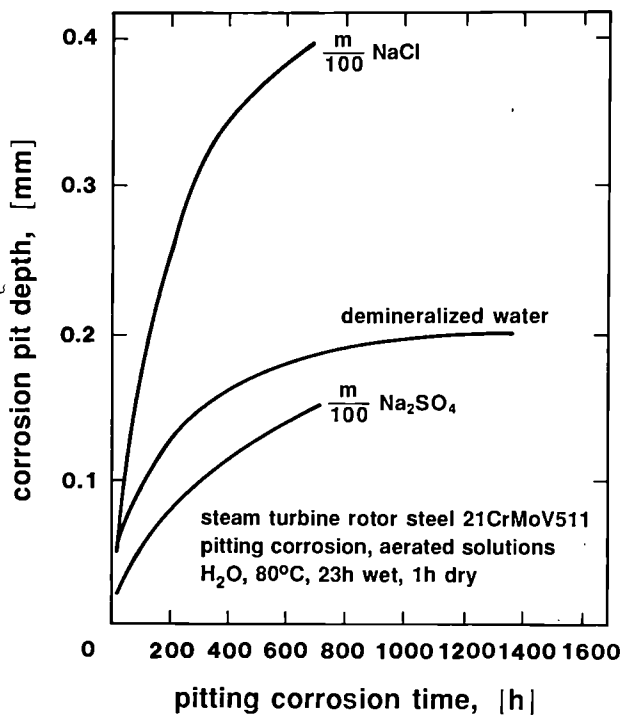


Fig. 40 The growth of corrosion pit depth with time in a steam turbine rotor steel exposed to water and aqueous solutions, /34/. Note that in demineralized water pits take up to one thousand hours to grow up to 0.2 mm in depth.

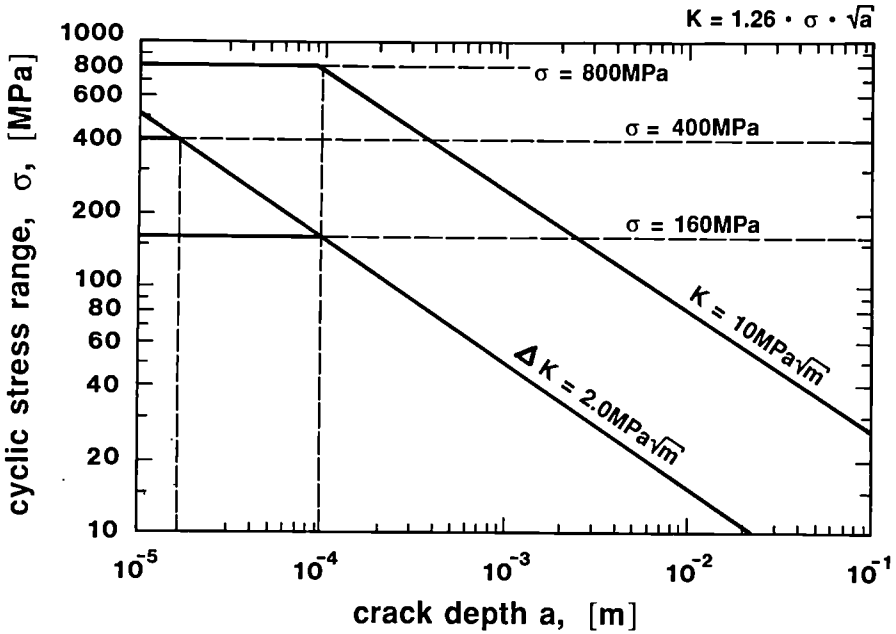


Fig.41 Stress corrosion and corrosion fatigue crack growth from corrosion pits - a fracture mechanics analysis. Note that cracks may grow by stress corrosion cracking or by corrosion fatigue from active pits when these reach about 100 μm depth.
(K formular for a semicircular surface crack with radius a)



European Communities — Commission

EUR 13186 — Stress corrosion cracking and corrosion fatigue of steam-turbine rotor and blade materials

Edited by: *J. B. Marriott*

Luxembourg: Office for Official Publications of the European Communities

1991 — V, 65 pp., num. tab., fig. — 16.2 x 22.9 cm

Physical sciences series

ISBN 92-826-2017-4

Catalogue number: CD-NA-13186-EN-C

Price (excluding VAT) in Luxembourg: ECU 6.25

Modern steam turbines must retain a very high reliability throughout their service life of typically 200 000 hours. Among the reasons for failure which have been observed in steam turbines during the last 20 years, stress corrosion cracking and corrosion fatigue have been prominent. Thus, attention has been drawn to the stress corrosion resistance and corrosion fatigue of steam-turbine rotor and blade materials.

The present paper summarizes and evaluates the present state of the art, mainly based on the results of the international cooperative research programme COST 505, recent literature and the authors' own experience.

An attempt is made to describe in quantitative terms the major influential parameters on stress corrosion and corrosion fatigue behaviour of steam-turbine rotor and blade materials in service-related environments.

Five topics are given special attention:

- (i) stress corrosion crack initiation,
- (ii) stress corrosion crack propagation,
- (iii) corrosion fatigue crack initiation,
- (iv) corrosion fatigue crack propagation,
- (v) pitting corrosion.

It is shown that fracture mechanics can be used to understand the transition from crack initiation to crack growth.



Venta y suscripciones • Salg og abonnement • Verkauf und Abonnement • Πωλήσεις και συνδρομές
Sales and subscriptions • Vente et abonnements • Vendita e abbonamenti
Verkoop en abonnementen • Venda e assinaturas

BELGIQUE / BELGIE

Moniteur belge /
Belgisch Staatsblad
Rue de Louvain 42 / Lauvenneeweg 42
1000 Bruxelles / 1000 Brussel
Tél. (02) 512 00 28
Fax 511 01 84
CCP / Postrekening 000-2005502-27

Autres distributeurs /
Overige verkooppunten

Librairie européenne/
Europese Boekhandel
Avenue Albert Jonnard 50 /
Albert Jonnardaan 50
1200 Bruxelles / 1200 Brussel
Tél. (02) 734 02 81
Fax 735 08 80

Jean De Lannoy
Avenue du Roi 202 / Koningaan 202
1000 Bruxelles / 1000 Brussel
Tél. (02) 538 51 89
Télex 63220 UNBOOK B

CREDOC
Rue de la Montagne 34 / Bergstraat 34
Bte 11 / Bus 11
1000 Bruxelles / 1000 Brussel

DANMARK

J. H. Schultz Information A/S
EF-Publikationer
Othlavej 18
2500 Valby
Tlf. 36 44 22 66
Fax 36 44 01 41
Girokonto 6 00 08 66

BR DEUTSCHLAND

Bundesanzeiger Verlag
Breite Straße
Postfach 10 80 06
5000 Köln 1
Tel. (02 21) 20 29-0
Fernschreiber:
ANZEIGER BONN 6 682 595
Fax 20 29 278

GREECE

G.C. Eleftheroudakis SA
International Bookstore
Nikis Street 4
10563 Athens
Tel. (01) 322 63 23
Telex 219410 ELEF
Fax 323 98 21

ESPAÑA

Boletín Oficial del Estado
Trafalgar, 27
28010 Madrid
Tel. (01) 446 80 00

Mundi-Pransa Libros, S.A.
Castelló, 37
28001 Madrid
Tel. (01) 431 33 99 (Libros)
431 32 22 (Suscripciones)
435 36 37 (Dirección)

Télex 46370-MPLI-E

Fax (01) 575 39 98

Sucursal:
Librería Internacional AEDOS
Consejo de Giento, 391
08009 Barcelona
Tel. (03) 301 66 16
Fax (03) 317 01 41

Generalitat de Catalunya:

Libreria Rambla dels estudis
Rambla, 118 (Palau Moja)
08002 Barcelona
Tel. (93) 302 88 35
302 64 82

FRANCE

Journal officiel
Service des publications
des Communautés européennes
26, rue Desaix
75727 Paris Cedex 15
Tél. (1) 40 58 75 00
Fax (1) 40 58 75 74

IRELAND

Government Publications

Sales Office

Sun Alliance House
Molesworth Street
Dublin 2
Tel. 71 03 09

or by post

Government Stationery Office

EEC Section

6th floor
Bishop Street
Dublin 8
Tel. 78 18 66
Fax 78 06 45

ITALIA

Licosa Spa
Via Benedetto Fortini, 120/10
Casella postale 552
50125 Firenze
Tel. (055) 64 54 15
Fax 64 12 57
Telex 570466 LICOSA I
CCP 343 509
Subagenti:
Libreria scientifica
Lucio de Bisalo - AEIDU
Via Meravigli, 16
20123 Milano
Tel. (02) 80 76 79

Herder Editrice e Libreria
Piazza Montecitorio, 117-120
00186 Roma
Tel. (06) 679 48 28/679 53 04

Libreria giuridica
Via XII Ottobre, 172/R
16121 Genova
Tel. (010) 59 56 93

GRAND-DUCHÉ DE LUXEMBOURG

Abonnements seulement
Subscriptions only
Nur für Abonnements

Messagerie Paul Kraus
11, rue Christophe Plantin
2339 Luxembourg
Tél. 499 88 88
Télex 2515
CCP 49242-63

NETHERLAND

SDU Uitgeverij
Christoffel Plantijnstraat 2
Postbus 20014
2500 EA 's-Gravenhage
Tel. (070) 378 98 80 (bestellingen)
Fax (070) 347 63 51
Telex 32488 strdu nl

PORTUGAL

Imprensa Nacional
Casa de Moeda, EP
Rua D. Francisco Manuel de Melo, 6
P-1092 Lisboa Codex
Tel. (01) 69 34 14

Distribuidora de Livros
Bertrand, Ld.*

Grupo Bertrand, SA
Rua das Terras dos Vales, 4-A
Apartado 37
P-2700 Amadora Codex
Tel. (01) 493 90 50 - 494 87 68
Telex 15798 BERDIS
Fax 491 02 55

UNITED KINGDOM

HMSO Books (PC 16)

HMSO Publications Centre
51 Nine Elms Lane
London SWB 5DR
Tel. (071) 873 9090
Fax GP3 873 6463
Telex 29 711 138

Sub-agent:

Alan Armstrong Ltd
2 Arkwright Road
Reading, Berks RG2 0SQ
Tel. (0734) 75 18 55
Telex 849637 AAALTD G
Fax (0734) 75 51 64

CANADA

Renouf Publishing Co. Ltd

Mail orders — Head Office:
1294 Algoma Road
Ottawa, Ontario K1B 3W8
Tel. (613) 741 43 33
Fax (613) 741 54 39
Telex 0534783

Ottawa Store:
61 Sparka Street
Tel. (613) 238 89 85

Toronto Store:
211 Yonge Street
Tel. (416) 363 31 71

JAPAN

Kinokuniya Company Ltd

17-7 Shinjuku 3-Chome
Shinjuku-ku
Tokyo 180-91
Tel. (03) 354 01 31

Journal Department

PO Box 55 Chitose
Tokyo 158
Tel. (03) 439 01 24

MAGYARORSZÁG

Agroinform

Központ:
Budapest I., Atilla út 63. H-1012

Lavelcim:
Budapest, Pf.: 15 H-1253
Tel. 36 (1) 56 82 11
Telex (22) 4717 AGINF H-61

ÖSTERREICH

Maria'sche Verlags-
und Universitätsbuchhandlung
Kohlmarkt 18
1014 Wien
Tel. (0222) 531 61-0
Telex 11 25 00 BOX A
Fax (0222) 531 61-81

SCHWEIZ / SUISSE / SVIZZERA

OSEK
Stampfenbachstrasse 65
8035 Zürich
Tel. (01) 365 51 51
Fax (01) 365 54 11

SVERIGE

BTJ
Box 200
22100 Lund
Tel. (046) 18 00 00
Fax (046) 18 01 25

TÜRKİYE

Dünya Süper Degitim Ticaret
ve sanayi A.Ş.
Narlıbashi Sokak No. 15
Cejajoluğu
İstanbul
Tel. 512 01 90
Telex 23822 DSVO-TR

UNITED STATES OF AMERICA

UNIPUB

4611-F Assembly Drive
Lanham, MD 20706-4391
Tel. Toll Free (800) 274 4888
Fax (301) 459 0058
Telex 7108260418

YUGOSLAVIA

Privredni Vjesnik

Bulevar Lenjina 171/XIV
11070 - Beograd
Yugoslavie

AUTRES PAYS
OTHER COUNTRIES
ANDERE LÄNDER

Office des publications officielles
des Communautés européennes
2, rue Mercier
L-2985 Luxembourg
Tél. 49 92 81
Télex PUBOF LU 1324 b
Fax 48 85 73
CC bancaire BIL 6-106/6003/700

NOTICE TO THE READER

All scientific and technical reports published by the Commission of the European Communities are announced in the monthly periodical '**euro abstracts**'. For subscription (1 year: ECU 84) please write to the address below.

Price (excluding VAT) in Luxembourg: ECU 6.25

ISBN 92-826-2017-4



OFFICE FOR OFFICIAL PUBLICATIONS
OF THE EUROPEAN COMMUNITIES

L-2985 Luxembourg

